Brain State Dependent Activity in the Lateral Geniculate Nucleus

PhD Thesis

Benedek Molnár

Supervisor:
Magor L. Lőrincz PhD

Doctoral School of Biology
Department of Physiology, Anatomy and Neuroscience
Faculty of Science and Informatics
University of Szeged

Szeged, 2021

TABLE OF CONTENTS

TABLE OF CONTENTS **2**

1. LIST OF PUBLICATIONS **3**

1.1. PUBLICATIONS RELATED TO THE SUBJECT OF THESIS 3

2. LIST OF ABBREVIATIONS **4**

3. INTRODUCTION **6**

3.1. HISTORICAL BACKGROUND 6
3.2. ROLE OF THE LATERAL GENICULATE NUCLEUS 8
3.2.1. Anatomy of the lateral geniculate nucleus *9*
3.2.2. Physiology of the lateral geniculate nucleus *11*
3.3. CELLULAR FUNCTION OF THE THALAMOCORTICAL CIRCUITRY 14
3.4. POPULATION LEVEL MECHANISMS OF STATE DEPENDENT THALAMOCORTICAL RHYTHMS 22
3.4.1. Delta rhythms (1–4 Hz) *24*
3.4.2. Slow waves (<1 Hz) *24*
3.4.3. Sleep spindles (7–14 Hz) *25*
3.4.4. Alpha (8–13 Hz) and theta waves (4–7 Hz) *25*
3.5. ROLE OF THE LATERAL HYPOTHALAMUS IN BRAIN STATES 28

4. AIMS **30**

5. MATERIALS AND METHODS **31**

5.1. SURGICAL PREPARATION 31
5.2. IN VIVO ELECTROPHYSIOLOGY AND JUXTACELLULAR LABELING 31
5.3. LOCAL PHOTOSTIMULATION OF LH AXONS IN THE DRN 33
5.4. CORTICAL INACTIVATION WITH MUSCIMOL 33
5.5. PUPILLOMETRY AND VISUAL STIMULATION 33
5.6. DATA ANALYSIS 34

6. RESULTS **36**

6.1. THE SPONTANEOUS ACTIVITY OF LGN IS CORRELATED WITH AROUSAL 37
6.2. THE MEMBRANE POTENTIAL OF LGN TC NEURONS IS CORRELATED WITH BRAIN STATES 41
6.3. VISUALLY EVOKED RESPONSES OF LGN TC CELLS 43
6.4. POPULATION-LEVEL ANALYSIS OF LGN NEURONS 44
6.5. CORTICOTHALAMIC MODULATION IS HINDERED BY VISUAL CORTEX INACTIVATION 45
6.6. LATERAL HYPOTHALAMUS AXONS INHIBIT GABAERGIC DRN NEURONS 46

7. DISCUSSION **48**

8. CONCLUSIONS **51**

9. ACKNOWLEDGEMENTS **53**

10. REFERENCES **54**

ABSTRACT **62**

ÖSSZEFOGLALÓ **63**

1. LIST OF PUBLICATIONS

1.1. Publications related to the subject of thesis

- **Benedek Molnár**, Péter Sere, Sándor Bordé, Krisztián Koós, Nikolett Zsigri, Péter Horváth, Magor L. Lőrincz (2021) Cell-type specific arousal-dependent modulation of thalamic activity in the lateral geniculate nucleus. *Cerebral Cortex Communications* **2**, 1–9. doi; 10.1093/texcom/tgab020

- Mary Gazea, Szabina Furdan, Péter Sere, Lukas Oesch, **Benedek Molnár**, Giuseppe Di Giovanni, Lief E. Fenno, Charu Ramakrishnan, Joanna Mattis, Karl Deisseroth, Susan M. Dymecki, Antoine R. Adamantidis, Magor L. Lőrincz (2021) Reciprocal lateral hypothalamic and raphé GABAergic projections promote wakefulness. *The Journal of Neuroscience* **41**(22) 4840-9; doi: https://doi.org/10.1523/JNEUROSCI.2850-20.2021

2. List of Abbreviations

ACh: acetylcholine

AP: action potential

AW: active wakefulness

EEG: electroencephalogram

EPSP: excitatory post-synaptic potential

FR: firing rate

GABA: gamma-aminobutyric acid

HCN: hyperpolarization-activated cyclic nucleotide-gated (channel)

HT(B): high-threshold (burst)

I_h: hyperpolarization-activated inward current

ISO: infra-slow oscillation

IT: T-type Ca2+-current

LC: locus coeruleus

LFP: local field potential

LGN: lateral geniculate nucleus

LH: lateral hypothalamus

LTCP: low-threshold Ca2+-potential

mAChR: muscarinic acethylcholine receptor

MEG: magnetoencephalography

MUA: multiunit activity

mGluR1a: metabotropic glutamate receptor 1a

NMDA: N-methyl-D-aspartate (receptor)

NREM: non-REM (sleep)

OB: olfactory bulb

OSI: orientation selectivity index

PB: phosphate buffer

PFA: paraformaldehyde

PV: parvalbumin

QW: quiet wakefulness

REM: rapid eye movement (sleep)

SOM: somatostatin

SS1: primary somatosensory cortex

TC: thalamocortical (cell)

TRN: thalamic reticular nucleus

V1: primary visual cortex

Vm: membrane potential

Additional abbreviations in figures are explicated in their corresponding captions.

3. INTRODUCTION

3.1. Historical background

Various states of vigilance, such as waking and sleep states, have been recognized in ancient cultures, being present in the Upanishads. After the rather confusing humoral theories of Aristotle, Lucretius exposes at length the Epicurean doctrine on sleep and on dreams (De rerum natura) explaining what happens during wakefulness and what is the reason why a prolonged waking state results in sleep. Several centuries needed to pass before scientists could realize and empirically confirm that sleep is yet another function of the brain (and the lack thereof), which can be measured as electrical signals by an electrode. The first electrical recording of brain activity was performed on animals by Richard Caton revealing its modulation by anesthesia and sensory responses (Haas, 2003). The term "electroencephalography" (EEG) was coined by Hans Berger, who recorded human brain waves in 1924 and consequently publishing his findings in 1929 citing Caton's valuable contribution to the field (Berger, 1929). Importantly, Berger noted that the activity patterns in the awake human brain differ in amplitude and frequency, depend on the behavioral state of the subjects, and classified them as alpha and beta waves occurring by closing and opening one's eyes, respectively (Berger, 1929).

Throughout the following decades, another field emerged in parallel with recording the summed activity of neuronal populations, namely, registering the sub- and suprathreshold electrical activity of individual neurons in various brain regions driven by the pioneering work carried out by Hodgkin and Huxley revealing the ionic mechanisms of the action potential in giant squid axons (Hodgkin & Huxley, 1939). Developments in the field brought the patch clamp method to life in the later decades, achieving high-fidelity registration of ionic currents through the neuronal membrane while also making high-end pharmacological experiments feasible. Methods of our days not only include recording individual neuronal activity in isolated brain slices but also whole-cell recording in vivo in either anesthetized or even awake animals. One of the most striking findings was published by Matteo Carandini's group, where whole-cell patch-clamp recordings of synaptic conductances revealed a surprising decrease in synaptic inhibition during anesthesia compared to wakefulness resulting in fewer visually-evoked spikes and briefer evoked responses during waking (Haider, et al., 2013). This leads to a more significant notion in terms of functional implication: the awake mammalian brain exhibits

higher spatial specificity to visual stimulation, since the ratio between the elicited response of center and surround stimuli is higher during wakefulness than under anesthesia (Fig. 1) This elevated inhibition during wakefulness reveals a regime of sensory processing that cannot be observed during anesthesia or sleep, where more balanced excitation and inhibition are evoked from large regions of space and persist long after the stimulus has disappeared. Enhanced inhibition in the awake cortex is ideally poised to extinguish any spatial or temporal spread of feedforward activity elicited by a sensory input. Accordingly, during wakefulness, a brisk and highly selective impulse response to spatially localized visual stimuli was observed (Haider, et al., 2013).

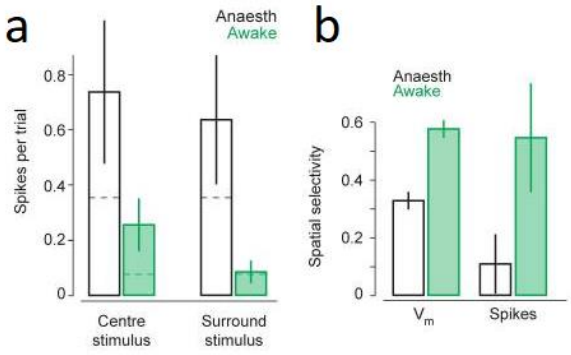

Figure 1. *Responses in awake mice were more selective across visual space.* A: Comparison of center and surround stimuli during wakefulness and under anesthesia. B: Quantified spatial selectivity of membrane potential and evoked spikes. (Haider, et al., 2013)

Brain states can fluctuate on various timescales and can profoundly influence neural and behavioral responses. Detailed observation of rapid state fluctuations can significantly account for variability and allow for a more accurate exploration of the neural mechanisms of behavior at all levels, from sensory coding to decision making and motor responses (McGinley, et al., 2015). This is most obvious when comparing spontaneous neuronal activity or responses to sensory stimuli between states of sleep and wakefulness (Livingstone & Hubel, 1981; Massimini, et al., 2005), but recently, the prominent influence of spontaneous variations within the waking state on both cortical neuronal responses and perceptual abilities has been documented in both humans (Fox & Raichle, 2007) and rodents (McGinley, et al., 2015). The latter study found coincident results and provides a thorough analysis of sensory information processing in cortical cells. Neocortical membrane potential has a signature of optimal sensory processing, a “sweet spot” corresponding to the highest level of selectivity specifically in mid-alert wakefulness. This was tested in mice performing an auditory detection task, resulting in

significantly lower performance both in relaxed and hyper-aroused states compared to mid-alert epochs, as indexed by pupil diameter (McGinley, et al., 2015). This phenomenon can be represented by an inverted U-shaped curve, a graph already invented and named "Yerkes-Dodson curve" after two psychologists, who studied cognitive performances of humans during various states of vigilance also indexed by pupil diameter, and found comparable results (Yerkes & Dodson, 1908). In the sections below, I would like to discuss in detail the various structures and features of the delicate systems that allow the mammalian brain to carry out these functions.

3.2. Role of the lateral geniculate nucleus

In my dissertation, I would like to focus on the thalamus, and in particular, the lateral geniculate nucleus (LGN). Anatomically, the thalamus is a nuclear complex located in the diencephalon

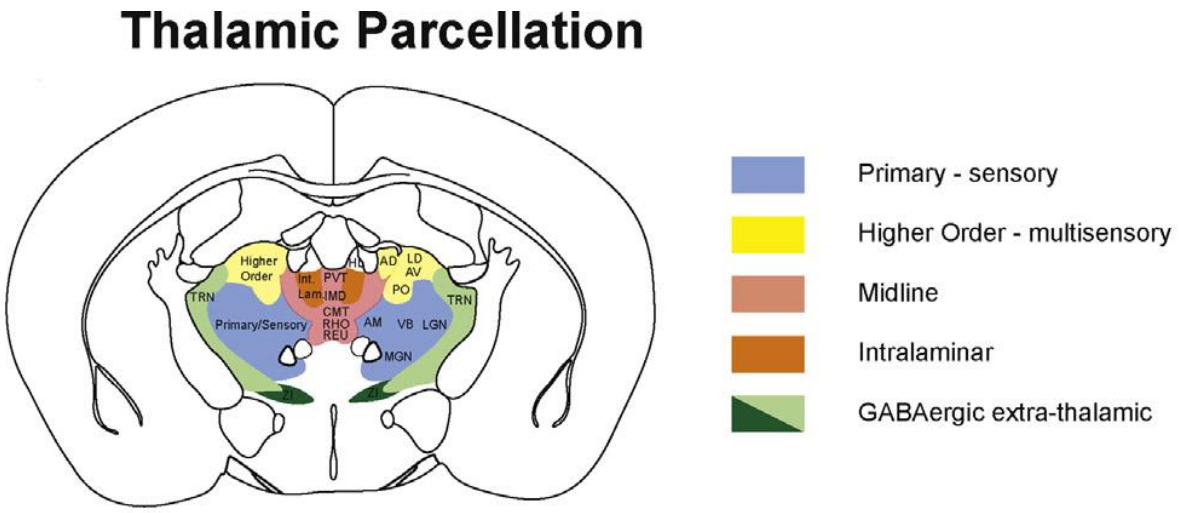

Figure 2. *Functional and anatomical regions of the thalamus*. Color coded regions of the thalamus (AD = anterodorsal; AM = anteromedial; AV = anteroventral; CMT = centromedial; IMD = intermediodorsal; LD = laterodorsal; LGN = lateral geniculate; MGN = medial geniculate; PO = posterior medial; PVT = paraventricular; REU = reuniens; RHO = rhomboideus; RTN = reticular thalamic; ZI = zona incerta). (Gent, et al., 2018)

and comprising of four parts (the hypothalamus, the epithalamus, the ventral thalamus, and the dorsal thalamus). Functionally, the thalamus is a relay center subserving both sensory and motor mechanisms. Thalamic nuclei (50–60 nuclei) project to one or a few well-defined cortical areas. Multiple cortical areas receive afferents from a single thalamic nucleus and send back information to different thalamic nuclei. The corticofugal projection provides positive feedback to the "correct" input, while at the same time suppressing irrelevant information (Herrero, et al., 2002). Sensory pathways (except the olfactory pathway) are relayed by specific thalamic

nuclei that all project to specific corresponding cortical areas, and in turn, receive exclusive and specific inputs from cortical areas (layer 6) to which it projects. Some thalamic nuclei do not receive sensory inputs, but instead are part of either higher-order associative corticothalamic circuitry, the midline and intralaminar thalamus and the extra-thalamic GABAergic reticular shell (Fig. 2). These are implicated in sensory information (secondary) integration, arousal and attention and the genesis of sleep spindles, respectively, (Gent, et al., 2018) into which I will delve deeper later.

3.2.1. Anatomy of the lateral geniculate nucleus

The lateral geniculate nucleus (LGN) is the visual relay nucleus of the thalamus, which is known to primarily taking input from the retinal ganglion cells (retinothalamic pathway) and after local processing, it projects visual information to layer 4 of the primary visual cortex (V1) (visual thalamocortical pathway) (Covington & Al Khalili, 2021). The LGN is also the point of origin for the optic radiations (Meyer's loop, central bundle, and Baum's loop) that project via the internal capsule to the primary visual cortex (V1), primarily synapsing onto spiny stellate neurons in layers 4C-alpha and 4C-beta. Analysis of LGN-dependent fMRI activity in non-V1 extrastriate cortex suggests that the LGN also projects to regions further downstream in the visual pathway (e.g., V2-5) (Covington & Al Khalili, 2021). While the LGN receives substantial input from the retinal ganglion cells, it receives far greater innervation from higher-order regions, such as modulatory feedback from layer 6 of V1 and the thalamic reticular nucleus (TRN) (Sherman & Guillery, 2002). It also receives varying degrees of modulatory activity from the raphe nuclei (serotonergic), (Yoshida, et al., 1984) pedunculopontine and laterodorsal tegmental nuclei (cholinergic) (Krueger & Disney, 2019), and locus coeruleus (noradrenergic) (Holdefer & Jacobs, 1994). The lateral geniculate nucleus also contains a distinct section between its dorsal and ventral regions known as the intergeniculate leaflet (IGL). The IGL projects to the suprachiasmatic nuclei of the hypothalamus via the geniculohypothalamic tract and to the pineal gland via the geniculopineal tract, implicating the LGN in the modulation of circadian/diurnal rhythms (Moore & Card, 1994). Historically, the lateral geniculate nucleus was highlighted for its role as little more than a signal repeater, however, subsequent research has suggested a more complex account of LGN function, including attentional modulation, temporal decorrelation, and binocular facilitation or suppression via monocular gain modulation (Covington & Al Khalili, 2021). Furthermore,

some research has suggested that a subpopulation of K cells in the LGN demonstrate selective sensitivity to stimulus orientation similar to V1 cells (Cheong, et al., 2013).

The traditional functional and morphological classification groups LGN cells into three morphological classes and three physiological classes. While the functional and morphological correspondence is not trivial due to the relatively high variability in morphology, the cells more or less fall into the categories demonstrated by Fig 3 (Friedlander, et al., 1981).

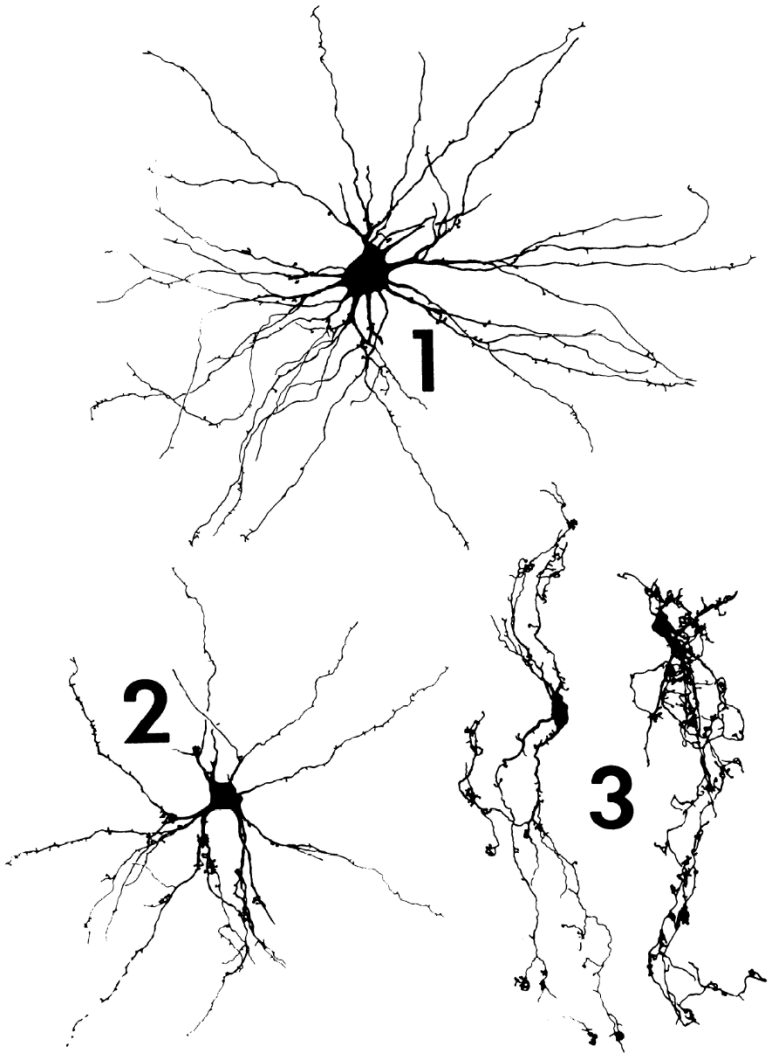

Figure 3. *Three major morphological classes of LGN cells*. The class 1 cell has a large soma and thick, cruciate dendrites with occasional, simple spinelike appendages. The class 2 cell has an intermediate-sized soma and dendrites of medium thickness with clusters of grapelike appendages near dendritic branch points. Two examples of class 3 cells are shown. They have small somata and thin sinuous dendrites with complex, stalked appendages. (Friedlander, et al., 1981)

Based on physiological features, there are W-cells, X-cells, and Y-cells (not to be confused with X- and Y-type retinal ganglion cells) chiefly relying on functional aspects, such as response latency to optic chiasm stimulation, linearity of spatial summation, and responsiveness to fast-moving targets (Friedlander, et al., 1981). While it seems logical to imagine that all functional (and structural) differences between X- and Y-cells are limited to the retina, if at least some of the morphological differences described for geniculate X- and Y-cells represent

the basis of functional differences in geniculate circuitry, then differences between the X- and Y-cell pathways are reinforced in the lateral geniculate nucleus, however, it is not necessarily the case. It is fair to assume that a class 1 neuron would be a Y-cell, a neuron with any class 3 features would be an X-cell, and a class 2 neuron could be identified either as an X- or Y-cell based on soma, dendrite, axon size, and the shape of the dendritic tree, and while most of these cells are relay cells (a.k.a. thalamocortical, or TC cells), a small portion of them do not project to the neocortex, but only have local postsynaptic targets, regardless of functional or morphological classification (Friedlander, et al., 1981).

3.2.2. Physiology of the lateral geniculate nucleus

The membrane potential of LGN cells has long known to be correlated with different brain states. During non-rapid eye movement (NREM) sleep the membrane potential is effectively hyperpolarized, and shows oscillatory activity with typical bursts, while the membrane potential becomes depolarized by 8–12 mV when the brain state is shifted to rapid eye movement (REM) sleep or to quiet wakefulness (Hirsch, et al., 1983). Not surprisingly, the average firing rate of LGN cells also increases during these transitions, which is caused by a tonic depolarization as suggested by Steriade (Steriade, 1978; Hirsch, et al., 1983).

What inputs shape the spontaneous activity of LGN cells specifically? As previously mentioned, geniculate cells receive input from various mesopontine nuclei of diverse neurochemical nature (cholinergic, noradrenergic, or serotonergic) either directly or indirectly through other modulatory areas, such as the TRN or neocortical layer 6. However, describing all known neuromodulators regulating geniculate cell and thalamocortical system function seems tempting, it exceeds the scope of this thesis, therefore I will restrain myself from elaborating every neuromodulatory impact in detail, and only focus on primary circuit function, the effect of acetylcholine, and the influence of dorsal raphe nucleus (DRN) and lateral hypothalamus (LH) on brain states, i.e., the phenomena I experimented with. Strikingly, while the major excitatory glutamatergic input to TC neurons in the LGN is originating from the retina, and cortical modulation was, intuitively enough, thought be conveyed through local GABAergic interneurons, studies have shown that cortical axons make twice the number of synapses on relay cells (i.e., TC cells) than on interneurons. An observation of high incidence of cortical (58%) versus retinal (12%) synapses on relay cells, emphasize a preponderant excitatory cortical influence on these cells (Montero, 1991). Furthermore, activation of corticothalamic fibers results in a slow depolarization of thalamic relay cells through reduction

of a potassium current through the activation of metabotropic glutamate receptors (slow EPSP) (McCormick & von Krosigk, 1992). This slow depolarization blocks rebound burst firing and promotes single spike activity, thereby promoting a state of thalamic activity that is associated with enhanced sensory transmission and arousal (McCormick & von Krosigk, 1992). The temporally prolonged nature of the corticothalamic slow EPSP suggests that this potential is probably involved in behavioral state changes that occur on the time scale of seconds or longer, whereas the ionotropic receptor-mediated fast corticothalamic EPSPs may be more important for the more phasic activation of thalamic excitability (McCormick & von Krosigk, 1992).

In terms of circuit physiology, the two types of thalamic inputs can also be classified as drivers and modulators. There are several characteristic features of drivers in the lateral geniculate nucleus that distinguish them from modulators. These characteristics include their fine structural appearance, their synaptic relationships, their degree of convergence on relay cells, their relatively small number relative to the modulators, their absence of connections to the thalamic reticular nucleus, their transmitter and receptor characteristics, and the nature of the cross-correlogram they produce when stimulated. Many of these properties are seen in all first order thalamic nuclei where the drivers can be identified. (Sherman & Guillery, 1998). There are two different functional states for thalamic nuclei. One involves the active, dynamic relay of driver activity to the cortex and characterizes the waking state. The other involves rhythmic, synchronized bursting of relay cells in which the relay cells no longer respond to driver inputs and are seen often during slow wave sleep (Sherman & Guillery, 1998). During this synchronized bursting, input from the thalamic reticular nucleus dominates relay cells, and excitatory postsynaptic potentials generated by driver inputs are insufficient to break the stranglehold of reticular inputs on thalamic relay cell responses, which is why effective thalamic relay functions are blocked during slow wave sleep. Note that the relay is disengaged not by silencing relay cells but, rather, by forcing these cells to burst rhythmically and independently of driver input. Thus, instead of silence, during slow wave sleep the neocortex receives synchronized, rhythmic excitatory bombardment from the thalamus. Silence alone would be ambiguous; the absence of a visual stimulus could not be distinguished from the absence of an effective relay of the stimulus. The rhythmic bursting, by signaling the “no-relay” alternative, avoids this ambiguity (Sherman & Guillery, 1998). Interestingly, cortical feedback mechanisms which regulate sensory information flow are not restricted to the thalamus but are also present in the olfactory bulb (OB). As it is long known, cortical regions underlying vision, audition, and somatosensation receive sensory information from the thalamus and also make

corticothalamic feedback projections that influence thalamic sensory processing. Thus, the cortex has the fundamental capacity to modulate the nature of its own input. In contrast to other sensory modalities, the olfactory system is unusual in that sensory information is initially processed in the olfactory bulb and conveyed directly (without a thalamic relay) to the olfactory cortex. Like the corticothalamic pathway, anatomical studies show that the axons of olfactory cortex pyramidal cells send abundant, long-range "centrifugal" projections back to the OB (Boyd, et al., 2012).

Sleep-wake cycles and other, more delicate brain state fluctuations during spontaneous mammalian behavior are also heavily reliant on neuromodulators, such as acetylcholine (ACh). The most prominent cholinergic input from laterodorsal tegmental and pedunculopontine nuclei make synaptic contact with F2 boutons of intraglomerular interneurons, which contribute to feed-forward inhibition to relay cells (Dolabela de Lima, et al., 1985). In the LGN, ACh can cause at least three different responses: fast nicotinic excitation, slow muscarinic excitation, and muscarinic inhibition (McCormick & Prince, 1987). The fast depolarizing action of ACh in (feline) geniculate neurons appears to be mediated by an increase in membrane conductance due to activation of nicotinic receptors. The muscarinic hyperpolarization of LGN neurons is due to the activation of a potassium conductance, and the hyperpolarizing action of ACh is not only proficient at inhibiting ongoing single-spike activity, but also has the ability to remove inactivation of the low-threshold Ca2+ current and thereby increase the probability of the occurrence of burst discharges. ACh-induced slow depolarizations result from the suppression of up to three different types of potassium conductances and associated currents: a voltage-dependent K+ conductance, a voltage-independent potassium conductance, and a calcium-activated K+ conductance (McCormick & Prince, 1987). The slow depolarizing response is perhaps the most interesting for it may mediate tonic depolarizations of relay cells which are observed during waking and REM sleep (Hirsch, et al., 1983). The muscarinic slow depolarization is mediated by a decrease in a K+ current which is active at rest (McCormick, 1993). Thalamic relay neurons exhibit two distinct firing modes: rhythmic burst firing during periods of drowsiness and slow wave sleep and single spike activity during waking and attentiveness. The muscarinic slow depolarization is effective in inhibiting rhythmic burst firing and promoting single spike activity by depolarizing the membrane potential the required 10-20 mV (McCormick, 1993). But how are inhibitory postsynaptic potentials decreased by activation of cholinergic fibers? Although one might imagine presynaptic inhibition of transmitter release, the answer is rather simpler. Application of ACh to identified GABAergic interneurons in either

the TRN or within the dorsal LGN itself results in inhibition of action potential activity through an M2-receptor-mediated postsynaptic increase in K+ conductance. This inhibition of inhibition (disinhibition) results in an increase in excitability of TC neurons and increased responsiveness to EPSPs arriving from the retina or visual cortex (McCormick, 1993).

3.3. Cellular function of the thalamocortical circuitry

In the absence of sensory input the mammalian brain exhibits a wide array of structured, brain state dependent spontaneous activity as happens during sleep (Steriade, et al., 2001; Lőrincz, et al., 2015) and relaxed wakefulness (Lőrincz, et al., 2009b; Crochet & Petersen, 2006; Lőrincz & Adamantidis, 2017). Slow waves and spindles occur largely during slow-wave sleep, while

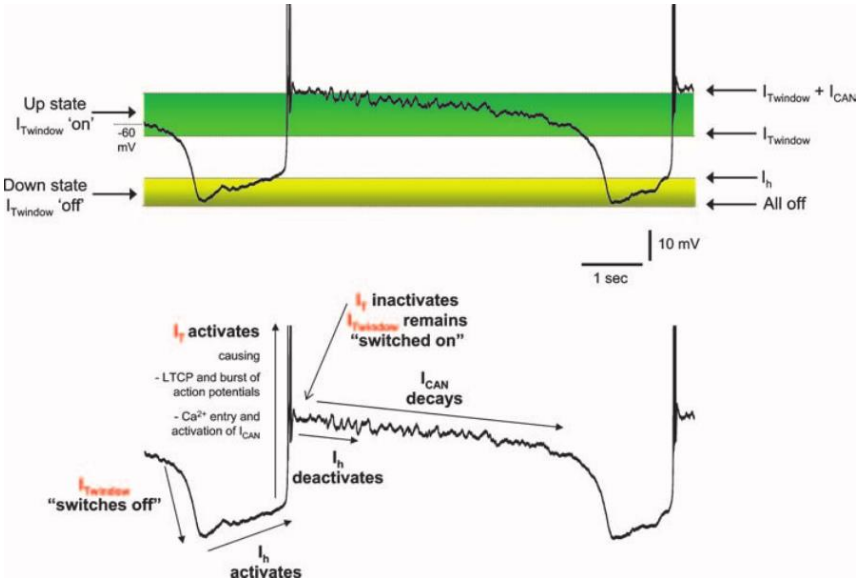

Figure 4. *Ionic mechanisms of the slow (< 1 Hz) sleep oscillation in TC neurons*. The presence of T-type Ca^{2+}-channel enable the dynamic alternation of „Up" and „Down" states in the thalamo-cortical network that accounts for slow-wave sleep shown by EEG (Crunelli, et al., 2004).

gamma waves are present throughout brain states, but are most prominent in the alert and attentive animal. Thalamocortical (TC) cells show membrane potential bistability that accounts for oscillatory activity. Low voltage-activated T-type $Ca2^{+}$ channels are important components of the large array of voltage-dependent membrane channels used by neurons to express different network dynamics (Crunelli, et al., 2004). The origin of the intrinsic bistability has been shown to involve an interaction between the steady-state ("window") component of low threshold, T-type Ca^{2+} current (I_T) (Hughes, et al., 1999). The primary contribution of the low threshold, transient Ca^{2+} current to the subthreshold electrical activity of central neurons has long been considered to be the low-threshold Ca^{2+} potential (LTCP). In a small group (15%) of

thalamocortical (TC) neurons, however, I_T is also responsible for an intrinsic bistability that manifests as: (i) input signal amplification, where responses to small current steps or synaptic potentials can be amplified in both the voltage and time domain when neurons are held in a membrane potential region centered around −60 mV, (ii) slow (0.1–1 Hz) oscillations appearing in NREM sleep with unusual plateau-like waveforms that differ substantially from conventional δ-oscillations, and (iii) in the absence of the hyperpolarization-activated inward current (I_h) membrane potential bistability, where two resting membrane potentials separated by up to 30 mV can exist for the same values of DC current and can be "switched" between by appropriate voltage perturbations (Fig. 4). This transition from the Down to Up state occurs when a strong enough (but not too strong) excitatory volley, either spontaneous or driven, enters into a local cortical network whose refractory mechanism has recovered sufficiently from the occurrence of the last Up state. The subsequent activation of excitatory neurons results in an amplification that initiates even more excitatory neurons to discharge, in a positive feedback loop (McCormick, et al., 2015). Owing to the buildup of refractory mechanisms, the recurrent networks become less able to maintain activity, and the network eventually and suddenly fails, resulting in a rapid transition to the Down state (Steriade, et al., 1993b). In terms of function, there is a classical view that they typically exhibit two modes of firing: an aforementioned interplay between various ionic currents can generate spontaneous rhythmic burst firing, whereas tonic firing is characterized by depolarized states (Jahnsen & Llinas, 1984). Traditionally, the waking state has been associated with an "activated" EEG, meaning a suppression of slow (<4 Hz) rhythmic activity, and an increased prevalence, either in absolute or relative terms, of higher frequencies, particularly in the gamma-frequency range (30-80 Hz). Recent intracellular recordings in waking mice have complicated this view, suggesting that rhythmic activity at 3-5 Hz can occur in the neocortex of head-restrained and stationary mice. This oscillatory activity is strongly suppressed by movement, such as walking or whisking (McCormick, et al., 2015). Extracellular and intracellular recordings from thalamocortical neurons during EEG-synchronized sleep in naturally sleeping animals revealed that these cells generate repetitive burst discharges that ride on top of a slower depolarizing potential (Hirsch, et al., 1983). The transition from EEG-synchronized sleep to the waking or REM-sleep states occurred with the progressive depolarization of thalamocortical cells and the abolition of the slow depolarizing spike and its associated burst of fast action potentials (McCormick & Bal,

1997). These alterations in the firing mode of thalamic neurons are associated with dramatic changes in the neurons' responsiveness to peripheral stimuli. For example, during slow wave sleep sleep, there is a marked diminution of the responsiveness of LGN thalamic neurons to activation of their receptive fields (Livingstone & Hubel, 1981), presumably owing to the hyperpolarized state of these neurons, the interrupting effects of spontaneous thalamocortical

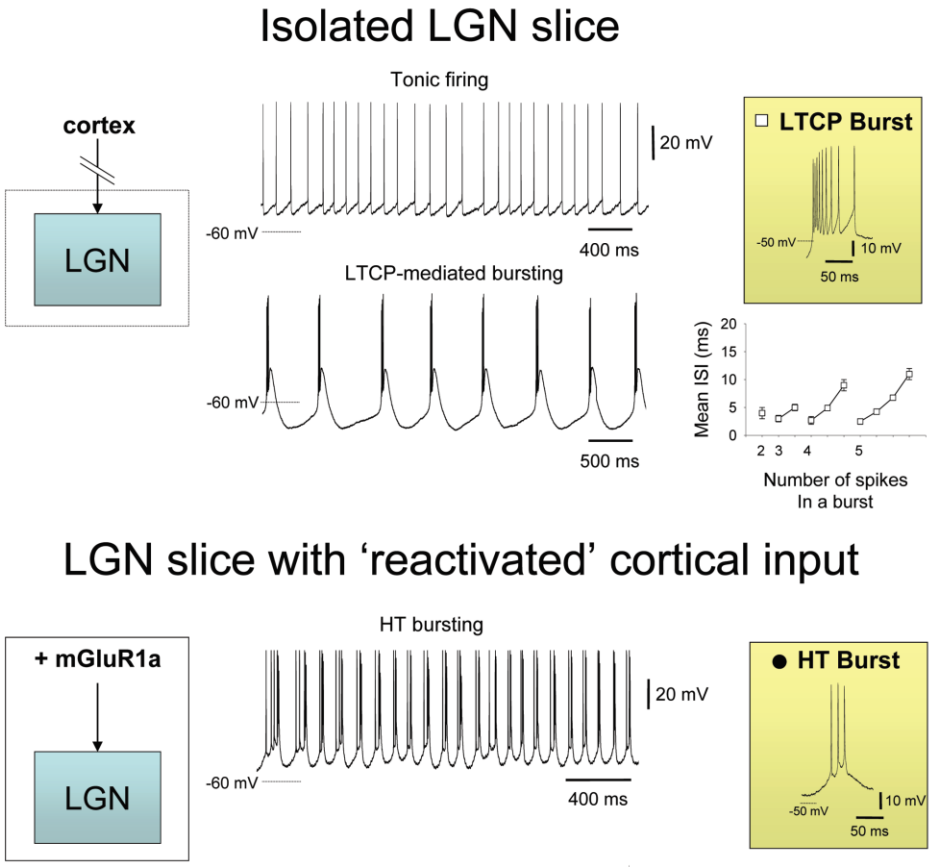

Figure 5. *Three firing modes of thalamocortical neurons.* In control conditions, thalamocortical (TC) neurons in the LGN exhibit 2 types of action potential output: tonic firing at depolarized membrane potentials and low-threshold Ca2+ potential (LTCP)–mediated burst firing at hyperpolarized membrane potentials (Jahnsen & Llinas, 1984; Leresche, et al., 1991). When corticothalamic feedback is reinstated by pharmacologically activating mGluR1a receptors TC neurons are subject to a persistent depolarization. In addition, a subset of these cells exhibits high-threshold (HT) bursting in addition to single spike activity (Hughes & Crunelli, 2005).

rhythms, and the frequency limitations of the burst firing mode (McCormick & Bal, 1997). Activation of the low-threshold calcium current, I_T, depolarizes the membrane toward threshold for a burst of Na^+- and K^+-dependent fast action potentials. The depolarization deactivates the portion of I_h that was active immediately before the Ca^{2+} spike. Repolarization of the membrane due to I_T inactivation is followed by a hyperpolarizing overshoot, which is due to the reduced depolarizing effect of I_h. The hyperpolarization in turn de-inactivates I_T and activates I_h, which depolarizes the membrane toward the threshold for another Ca^{2+} spike (McCormick & Pape,

1990). The kinetics of activation of I_T are considerably faster than are the kinetics of inactivation, similar to the Na^+ current underlying the generation of the more typical fast action potentials. Therefore, if the membrane potential is depolarized from a relatively hyperpolarized membrane potential (negative to −65 mV), then I_T may first activate and then more slowly inactivate, generating a low-threshold Ca^{2+} spike. These Ca^{2+} spikes typically last on the order of 100–200 ms, and in turn bring the membrane potential positive to threshold (approximately −55 mV) for the generation of a burst of three to eight fast action potentials (Jahnsen & Llinas, 1984). Intracellular recordings of TC neurons reveal that this firing behavior is generated by a novel form of burst firing, which occurs at relatively depolarized (>–55 mV) membrane potentials and which has been termed high-threshold (HT) bursting (Fig. 5) (Hughes, et al., 2002).

It is well-known that the membrane potential of LGN neurons is dependent on brain state (Hirsch, et al., 1983). A fundamental study carried out in cats indicates that the fast discharge of REM sleep is related to a tonic depolarization as previously suggested and not to an increase of the amplitude of individual EPSPs. The change of membrane potential toward a more polarized state as the animal shifted from quiet waking to NREM sleep and the similarity between the spontaneous large amplitude depolarizations of NREM sleep and those which resulted from intracellular injection of hyperpolarizing currents during drowsiness suggest that LGN relay neurons are subjected to a tonic hyperpolarization during the later stage of NREM sleep (Hirsch, et al., 1983). During wakefulness, the brain constantly fluctuates between transient states that differ in EEG wave components as well as in subthreshold potentials of individual neurons constituting an oscillatory network (Crochet & Petersen, 2006; Poulet & Petersen, 2008; Bennett, et al., 2013; Zagha, et al., 2013; McCormick, et al., 2015; McGinley, et al., 2015). Recent studies implicate that sensory performance also varies in accordance with these state transitions (Bennett, et al., 2013; Vinck, et al., 2015; Reimer, et al., 2014; Polack, et al., 2013). In addition, locomotion modulates sensory coding in the primary somatosensory (SS1) (Zagha, et al., 2013) and primary visual cortices (V1) (Polack, et al., 2013). As previously mentioned, a key brain area in both the transmission of visual information and the generation of the α rhythm is the LGN (Hughes, et al., 2004; Hughes & Crunelli, 2005). In this structure, a specialized subset (∼25%–30%) of TC neurons exhibit intrinsic rhythmic burst firing at α frequencies (HT bursting), which occurs coherently with naturally occurring α waves *in vivo* (Hughes, et al., 2004; Hughes & Crunelli, 2005) and which can be synchronized by gap junctions (GJs), i.e., electrical synapses, to form an α rhythm pacemaker unit (Lőrincz, et al.,

2008). While the strong intrinsic rhythmicity of these cells is ideally suited to driving thalamic and cortical α oscillations, it is generally accepted that the faithful transmission of visual information from the retina to the neocortex is carried out by the conventional single spike or so-called relay-mode of firing that occurs in the remainder and overwhelming majority of LGN TC neurons (Llinás & Jahnsen, 1982). Naturally occurring α rhythms actively and discretely constrain the temporal dynamics of neurons that directly carry out the transmission, and influence the processing, of early-stage visual information (Lőrincz, et al., 2009b).

In cortical areas state dependent neuronal activity is determined by both thalamic (Poulet, et al., 2012) and neuromodulatory inputs (Constantinople & Bruno, 2011; Eggermann, et al., 2014; Reimer, et al., 2016). In the thalamus, thalamocortical and thalamic reticular neurons show state dependent membrane potential alterations leading to altered modes of rhythmic firing ranging from LTCP-mediated burst firing during NREM sleep (Hirsch, et al., 1983), tonic firing and HTB firing during active and quiet wakefulness, respectively (Hughes, et al., 2004; Lőrincz, et al., 2009b; Crunelli, et al., 2018). The near ubiquitous presence of low-threshold and high-threshold spikes in TC and TRN neurons during low-vigilance states raises the question of why individual thalamic neurons are paradoxically engaged in the energetically expensive generation of rhythmic burst firing during periods of attentional and behavioral inactivity that are classically associated with energy preservation (Crunelli, et al., 2018). In the nearly 90 years since the first description of a physiologically relevant rhythm in the human EEG (Berger, 1929), considerable effort has been directed towards gaining a deep understanding of the mechanisms and physiological importance of EEG waves. The complex picture that has emerged reveals that although the source of the EEG signals resides within the neocortical supragranular layers, the rhythm generators of different EEG waves are found within both the neocortex and thalamus (Crunelli, et al., 2018). Intrinsic and network generators exist in both the neocortex and the thalamus, which are capable of locally eliciting oscillations at alpha (8–13 Hz), theta (4–7 Hz), spindle (7–14 Hz), slow (<1 Hz) and delta (0.5–4 Hz) frequency (summarized in Fig. 6). However, simply on the basis of the structurally widespread and functionally powerful reciprocal connections between the neocortex and thalamus, it would be unreasonable to argue that the alpha, theta, spindle, slow and delta rhythms recorded in the EEG during low-vigilance states solely and uniquely rely on the rhythm-generating processes of one of these brain regions without any contribution from the other. Indeed, in all studies where this question has been directly addressed under unrestrained fully behaving conditions, the EEG rhythms of low-vigilance states have been found to be either modulated, regulated or controlled

(to various degrees and in different properties) by the neocortex and/or thalamus (Crunelli, et al., 2018). Thus, as neocortical dynamics affect oscillations generated in the thalamus, so does thalamic activity influence neocortically generated waves, with these interactions facilitating and/or reinforcing the overall synchrony in large thalamic and cortical neuronal population. Notably, the extent of this rhythm-regulation function of thalamic low-vigilance state oscillations varies greatly among different EEG rhythms, ranging from the strong rhythm imposed on the neocortex by the thalamically generated sleep spindles to the more subtle thalamic modulation of slow oscillations recorded in the neocortex (Crunelli, et al., 2018).

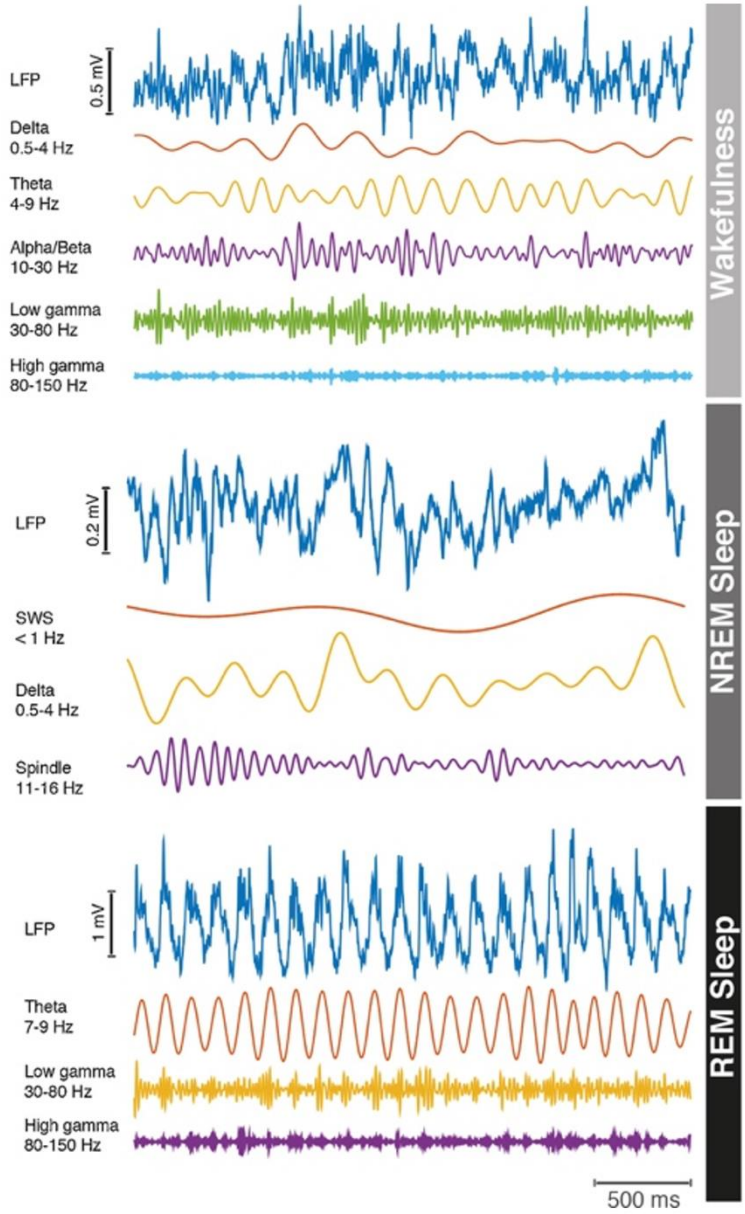

Figure 6. *Summary of sleep-wake states in the rodent brain.* Filtering decomposition of LFP/EEG signals across sleep-wake states in freely moving mice (Lőrincz & Adamantidis, 2017).

Additionally, infra-slow oscillation (ISO) is another noteworthy brain function with a periodicity of tens of seconds to a few minutes, alas, under-investigated feature of macroscopic brain activity (Lőrincz, et al., 2009a). Such oscillations were first observed in LFP recordings

from the rabbit neocortex but have since been observed in several other mammals and are readily detectable in full band EEG recordings from humans (Hughes, et al., 2011). ISOs are also a consistent and important feature of the fMRI BOLD signal during the resting state, or so-called default mode, in humans and in anaesthetized nonhuman primates and rats (Vanhatalo, et al., 2004). The emerging functions of ISOs include a role in modulating gross neuronal excitability, being correlated with fluctuations in the amplitude of faster EEG oscillations in several well-defined frequency bands in the 1–80 Hz range, and in regulating behavioral performance (Lőrincz, et al., 2009a). Although the origins of ISOs are not well understood, recent EEG and imaging studies in humans support a key involvement of subcortical structures and, in particular, the thalamus (Vanhatalo, et al., 2004). In humans these oscillations identify highly specific functional anatomical networks (termed resting state networks), some of which are thought to involve a significant contribution from the thalamus (Lőrincz, et al., 2009a). These observations have several functional implications in terms of awake brain activity and is well studied in rodents. Slow synchronous fluctuations in EEG, local field potential, and membrane potential of L2/3 barrel cortex neurons are prominent during quiet wakefulness in relaxed head-restrained mice (Crochet & Petersen, 2006). During whisking, when the mouse is actively scanning its immediate environment, these slow membrane potential fluctuations are suppressed. Membrane potential variance is decreased, and the remaining membrane potential fluctuations become less correlated in nearby neurons (Fig. 7A) (Poulet, et al., 2012). The reduced membrane potential variance during whisking might help improve signal-to-noise ratios for sensory processing (Poulet & Petersen, 2008). The cortical state change during whisking is not affected by cutting the peripheral sensory nerves innervating the whisker follicle, suggesting that the active desynchronized cortical state is internally driven by the brain (Poulet & Petersen, 2008). The desynchronized cortical state in primary somatosensory cortex during whisking is correlated with an increased firing rate of thalamocortical cells, is blocked by pharmacological inactivation of the thalamus, and can be mimicked by optogenetic stimulation of the thalamus (Fig. 7B) (Poulet, et al., 2012). Thus, an increase in thalamic firing rate drives important aspects of the cortical state change during whisking (Poulet, et al., 2012).

Neuromodulatory inputs are also likely to play a significant role in generating some desynchronized brain states (Constantinople & Bruno, 2011; Petersen & Crochet, 2013).

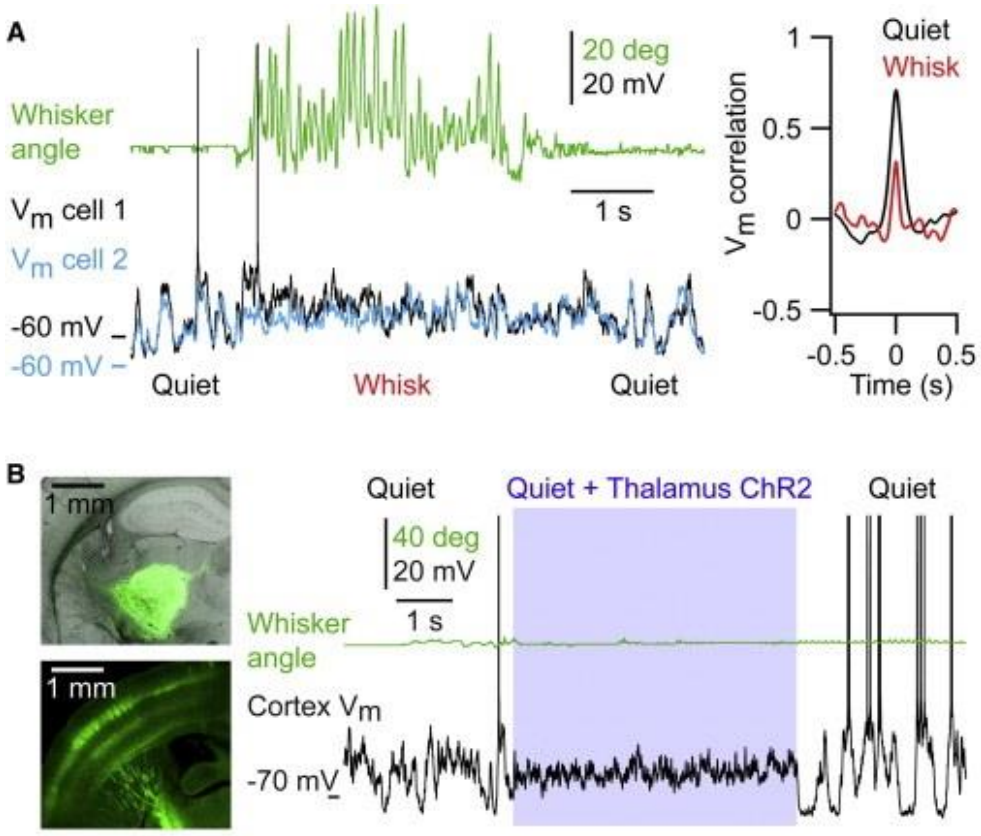

Figure 7. *Cortical neuron membrane potential correlates with brain states.* (A) Simultaneous whole-cell patch-clamp recording of two L2/3 neurons from the barrel cortex of an awake mouse during quiet wakefulness and whisking behavior (green, whisker position; black and blue, membrane potentials). Right: slow, large Vm fluctuations were highly correlated in the two neurons during quiet wakefulness (black), whereas the fast, small-amplitude Vm fluctuations during whisking were less correlated (red) (Poulet & Petersen, 2008). (B) Optogenetic stimulation of somatosensory thalamus drives cortical desynchronization. Left: epifluorescence images showing the expression of ChR2-Venus in the somatosensory thalamus (top) and in thalamocortical axons projecting to the barrel cortex (bottom). Right: an example whole-cell recording in the barrel cortex of an awake mouse during quiet wakefulness before, during, and after optogenetic stimulation of the thalamus (blue shaded period) (Poulet, et al., 2012).

Brain state changes are sometimes coupled with overt movements such as whisking or locomotion and can also be predicted with high accuracy by changes in pupil diameter or muscle tone while animals are sitting quietly. Classically, slow wave sleep is characterized by a high density of cortical field potential power at 0.5–4 Hz, and reduced muscle tone, while waking is associated with a relative suppression of low frequency activity (usually termed "activation" or "desynchronization"), increased muscle tone, and behaviorally relevant eye movements (e.g. fixation, saccades, and smooth pursuit) (McGinley, et al., 2015). All together, these biomarkers for waking states predict changes in the capability of animals to represent and respond to

stimuli, and account for a significant fraction of the variability in spontaneous and stimulus-driven activity and behavior (McGinley, et al., 2015).

Over the last 50 years, waking brain state has been assessed in psychophysical experiments by monitoring the diameter of the pupil (Kahneman & Beatty, 1966). Human and animal studies have shown that changes in pupil diameter (after controlling for changes associated with luminance and depth accommodation) are correlated with arousal, attention, emotion, cognitive perception, "brain gain", as well as heart rate and galvanic skin reflex, indicating a tight coupling between the state of the central and peripheral nervous systems (Kahneman & Beatty, 1966) (McGinley, et al., 2015). Recently, intracellular membrane potential (V_m) and local field potential (LFP) recordings from cortical neurons collected simultaneously with pupil diameter in head-restrained, spontaneously locomoting or whisking mice revealed a marked relationship between pupil size, low frequency (2–10 Hz) fluctuations in membrane potential/LFP, and exploratory behaviors (whisking and locomotion) (McGinley, et al., 2015; Reimer, et al., 2014; Vinck, et al., 2015). Moreover, human intracranial and magnetoencephalographic (MEG) data show that retinal inputs are temporally aligned to a preferential alpha phase which are consistently preceded by saccadic eye movements (Staudigl, et al., 2017). Importantly, this coordination of saccades was related to successful memory encoding, suggesting a mechanistic role for alpha oscillations in coordinating the encoding of visual information. Furthermore, these data point to an active involvement of task-relevant brain areas in this coordination: MEG and intracranial data yielded the occipital cortex, the parahippocampal gyrus, and the retrosplenial cortex as sources of the coordination of saccades and alpha phase, which have been shown to support the encoding of visual scenes (Kravitz, et al., 2011).

3.4. Population level mechanisms of state dependent thalamocortical rhythms

The human electroencephalogram (EEG) expresses a range of distinctive waves, progressively increasing in amplitude and decreasing in frequency, the most prominent of which are the alpha rhythm, sleep spindles, delta waves and slow waves (Niedermeyer & Lopes Da Silva, 2004) (summarized in Figure 8). The emergence of these EEG rhythms is reliant upon finely tuned interactions between neocortical and thalamic neuronal assemblies, with strong modulation

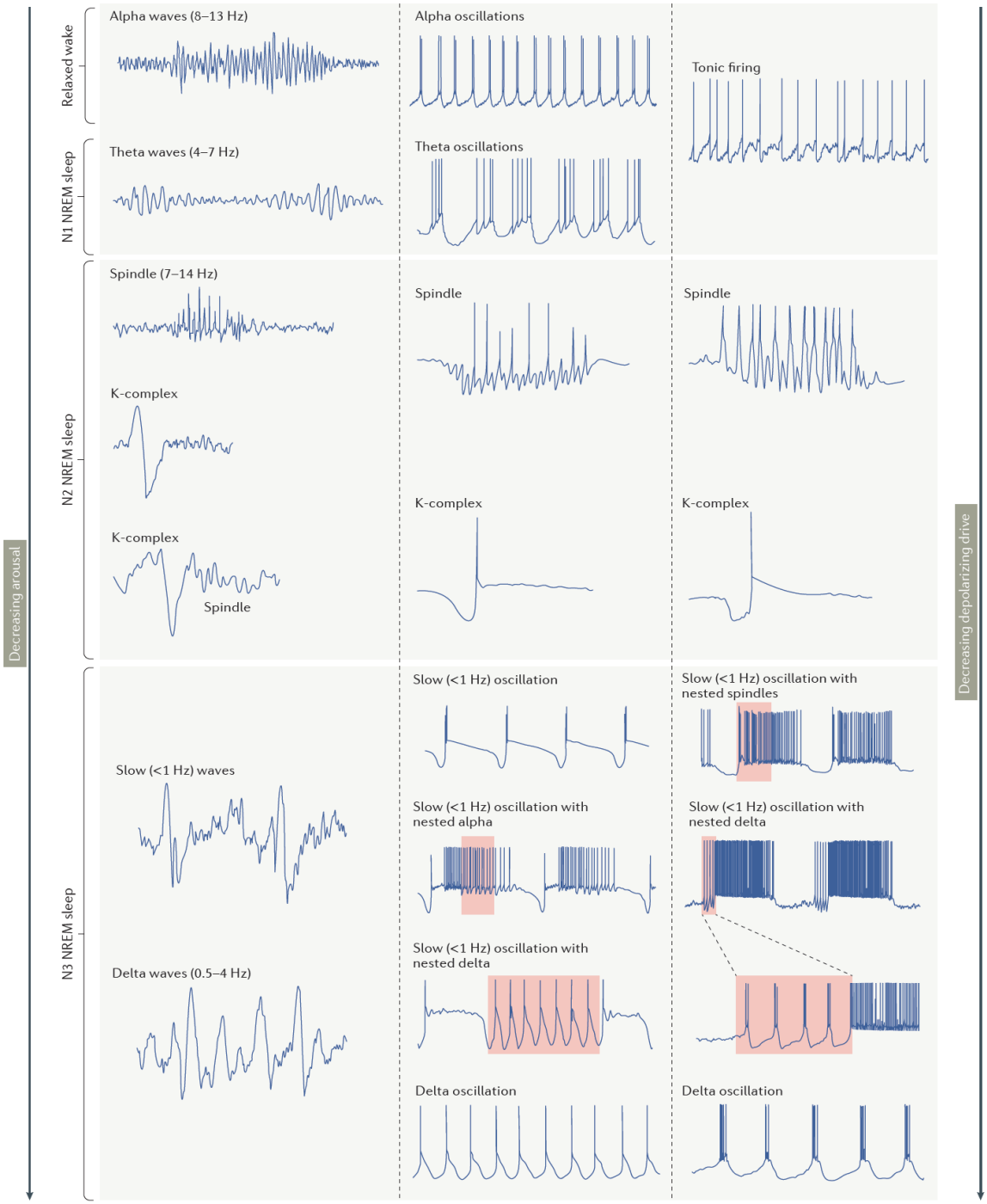

Figure 8. *Cellular thalamic counterparts of electroencephalogram rhythms of relaxed wakefulness and non-rapid eye movement sleep.* Representative intracellular recordings from TC (middle column) and TRN (right column) neurons depicting the membrane potential changes occurring in these neurons during the respective EEG rhythms shown in the left column (N1–N3: NREM sleep stages). Sleep spindles can occur in isolation or following a K-complex. A K-complex in the EEG results from a single cycle of the slow (<1 Hz) oscillations. In the TC neuron column, pink boxes highlight alpha and delta oscillations nested in the UP and DOWN state, respectively, of slow (<1 Hz) oscillations in N3. In the TRN neuron column, pink boxes highlight spindle waves in the UP state and delta oscillations in the DOWN state, respectively, of slow (<1 Hz) oscillations in N3. TRN neurons do not express firing coherent with alpha and/or theta waves (wake state and N1). Action potentials in the traces depicted in the middle and right column have been truncated for clarity of illustration. (Crunelli, et al., 2018)

from many subcortical regions, including the brainstem and hypothalamus (Herrera, et al., 2016; Lőrincz & Adamantidis, 2017).

3.4.1. Delta rhythms (1–4 Hz)

The isolated neocortex expresses delta oscillations due to certain pharmacological manipulations whereby the neuromodulatory tone is reinstated giving rise to powerful reciprocal excitation of layer 5 intrinsically bursting neurons (Carracedo, et al., 2013; Lőrincz, et al., 2015). Most TC neurons and NRT neurons, can exhibit a few cycles of delta oscillations in vivo, whereas persistent delta oscillations are observed in decorticated animals (Dossi, et al., 1992; Timofeev & Steriade, 1996). In contrast to the neocortex, delta oscillations in thalamic neurons are generated by cell-intrinsic mechanisms, namely by the dynamic interaction of I_T and I_h in TC neurons (McCormick & Pape, 1990; Leresche, et al., 1991) and Ca^{2+}-activated K^+ currents in TRN neurons forms the pacemaker mechanism that enables individual thalamic neurons to elicit LTS-bursts at delta frequency (Bal & McCormick, 1993). Presumably, the relative contribution of the neocortex and thalamus to EEG delta waves of natural sleep, the presence of delta frequency generators in both brain regions suggests that both the neocortex and thalamus have a role in producing this EEG rhythm (Crunelli, et al., 2018).

3.4.2. Slow waves (<1 Hz)

The most prominent EEG component of NREM sleep, hence the name "slow wave sleep" is used in synonymy with NREM sleep. Jointly with delta waves, EEG waves of stage 3 of NREM (N3) sleep contain slow (<1 Hz) waves as well. Slow waves reflect the rhythmic alternation of so-called depolarized Up and hyperpolarized Down states observed in almost all neocortical and thalamic neurons so far investigated in vivo and in vitro (Steriade, et al., 1993b; Steriade, et al., 1993a; Hughes, et al., 2002; Lőrincz, et al., 2015). Whereas both the neocortex and thalamus in isolation have different generators of slow oscillations the full expression of sleep slow waves in the EEG requires active thalamic participation (Lemieux, et al., 2014). While this activity is primarily generated by the interaction between synaptic excitation and inhibition in the neocortex (Lőrincz, et al., 2015), in TC neurons on the other hand, slow oscillations are generated by a cell-intrinsic mechanism that requires the cooperation between the leak K^+ current, the T-type voltage gated calcium "window current" ($I_{Twindow}$), the Ca^{2+}-activated non-selective cation current (I_{CAN}) and the HCN current by hyperpolarization-activated cyclic nucleotide-gated (HCN) channels (Crunelli, et al., 2004) (Fig. 4).

3.4.3. Sleep spindles (7–14 Hz)

Sleep spindles are global EEG waves of NREM stage N2 generated in the thalamus characterized by a typical waxing and waning temporal profile (Steriade, et al., 1985). These typical oscillations are generated by a mutual synaptic interaction between excitatory TC and inhibitory NRT neurons (Bal, et al., 1995; Bal, et al., 1995). Although the neocortex cannot generate sleep spindles in the absence of the thalamus as elimination of the thalamic input to the neocortex abolishes spindles in the EEG during natural sleep (Steriade, et al., 1985), the corticothalamic feedback to TC and NRT neurons provides essential contributions to some sleep spindle properties (Contreras, 1996).

3.4.4. Alpha (8–13 Hz) and theta waves (4–7 Hz)

Alpha waves were the first EEG rhythms to be recorded (Berger, 1929) and they are present in the EEG during relaxed inattentive wakefulness, that is, in the behavioral state that falls between fully attentive wakefulness and stage N1 of NREM sleep, and also during attentive perception (Crunelli, et al., 2018). Although, the mechanisms underlying the alpha waves of these two behavioral states might be different, I am going to focus on those occurring during inattentive wakefulness, because based on our experiences, the quiet wakefulness behavior of mice resembles this alpha oscillation. Theta waves that are present in the EEG of humans and higher mammals during stage N1 of NREM sleep have a similar mechanism of generation as alpha waves (Hughes, et al., 2004). Both waves are driven by a subset of gap junction-coupled TC neurons that generate high-threshold bursts (HTB) phase-locked to each cycle of the corresponding EEG rhythm (Hughes, et al., 2004) (Fig 5). HTBs in TC neurons entrain the firing of local thalamic interneurons and other non-HT-bursting TC neurons, giving rise to a thalamic output at alpha or theta frequency, depending on the behavioral state (Lőrincz, et al., 2009b). From a functional perspective, inhibition of HTBs within a small (<1 mm^3) area of lamina A of the dorsal LGN in freely moving cats markedly, selectively and reversibly decreases alpha waves in the surrounding thalamic territory and in the EEG recorded from the primary visual cortex by 90% and 75%, respectively (Lőrincz, et al., 2009b). A substantial body of evidence suggests that LGN α rhythms and related TC neuron firing require thalamic activation of muscarinic acetylcholine receptors (mAChRs) (Lőrincz, et al., 2008) and/or metabotropic glutamate receptor 1a (mGluR1a) (Hughes, et al., 2004). In vivo reverse microdialysis experiments confirmed a role for these receptors but also showed that LGN α rhythms are considerably more susceptible to blocking mAChRs than to antagonizing

mGluR1a, indicating that they are mainly reliant on a cholinergic drive (Lőrincz, et al., 2009b). Consistent with this, intracellular recordings of relay-mode LGN TC neurons, obtained in vitro during α rhythms that had been induced by reinstating the cholinergic drive with the nonspecific AChR agonist carbachol (Lőrincz, et al., 2008), revealed a pattern of action potential output almost identical to that observed in vivo (Lőrincz, et al., 2009b).

So far, I have discussed the thalamus as sole generator of alpha and theta rhythms, but the existence of neocortical rhythm generators cannot be excluded, since many studies in vivo provide indirect support for a cortical involvement in classical EEG alpha waves (Lopes da Silva, et al., 1980; Lopes Da Silva & Storm Van Leeuwen, 1977; Bollimunta, et al., 2011; Halgren, et al., 2019). Thus, whereas the precise nature of neocortical alpha-generating networks is at present not clear, it is reasonable to suggest that the alpha and theta waves that characterize the EEG of relaxed, inattentive wakefulness and N1 NREM sleep, respectively, are strongly, though not exclusively, driven by the thalamic HTB-generating mechanism described above (Crunelli, et al., 2018).

A good example of neocortical alpha-generation is "striate" visual alpha rhythm that manifests in local circuits of V1 following periods of slow gamma-frequency activity (Traub, et al., 2020). Recent findings revealed a number of similarities with the phenomenon as studied non-invasively in human subjects: it required a prior period of excitatory (sensory) activity; it was time-limited, fading as time from this prior excitation increased; it was abolished on subsequent re-establishment of excitation (sensory input); it was sensitive to NMDA receptor blockade (Vlisides, et al., 2018); its primary generation mechanism appeared to be largely synaptic inhibition-independent (Lozano-Soldevilla, et al., 2014). Complex bursts from main branches of pyramid apical dendrites occur via voltage-operated calcium channel conductances, whereas bursts mediated by NMDA receptors are seen on finer dendritic processes (Nevian, et al., 2007). Both have a role in synaptic integration and together have been shown to powerfully influence sensory processing (Larkum, et al., 2009). Although non-synaptic dendritic bursting is apparent in L4 pyramidal neuron recordings, no involvement of individual voltage-operated calcium channel subtypes was observed to contribute to the alpha rhythm (Traub, et al., 2020). This may indicate the involvement of a complex admixture of channel subtypes or a dominant involvement of NMDA spikes. Both the bursts and the alpha rhythm were dependent on blockade of hyperpolarization-activated conductance I_h (Traub, et al., 2020). The latter intrinsic conductance state is essential for generating dendritic NMDA bursts, suggesting the change in dendritic electrogenesis essential for alpha-rhythm generation was almost entirely mediated by

NMDA receptor-dependent synaptic excitation, a factor that may also contribute to the strong local synchrony inherent in the LFP alpha-rhythm recordings (Traub, et al., 2020). By analyzing laminar profiles of LFP and multiunit activity (MUA) recorded with linear array multielectrodes from the visual cortex of behaving macaque monkeys a study found separate alpha current generators located in superficial, granular, and deep layers, respectively (Bollimunta, et al., 2011). This study also confirmed that alpha oscillations in the lateral geniculate cohere with those in V1. During visual stimulation, alpha-range field potentials are strongly coupled with spiking throughout the cortical column but especially in supragranular layers (Dougherty, et al., 2015). The strongest alpha-locked sink in deep layers below the layer 4C/5 border at the time of alpha troughs. At counter-phase (coincident with deep layer alpha peaks), the sign of the sinks and sources reversed so that a sink was present in the granular layer. The alpha-locked current source density patterns suggest endogenous activation of granular and infragranular compartments that alternates at a low frequency (~7–14 Hz) (Dougherty, et al., 2015). Moreover, LFP and spike recordings from macaques performing a somatosensory discrimination task corroborated these findings as it has been demonstrated that the decrease of alpha power across sensorimotor cortices correlated with better discrimination performance (Haegens, et al., 2011). Furthermore, it has been shown that the alpha rhythm interacts with spike activity: firing rate goes up when alpha power goes down and the neuronal firing is strongly related to the phase of ongoing alpha oscillations (Haegens, et al., 2011). Despite the lack of classical alpha rhythms in rodents stereotyped 3–5 Hz V_m and LFP oscillations can be recorded (Einstein, et al., 2017) possessing several similarities with the alpha oscillations recorded in primates and felines (Senzai, et al., 2019).

3.5. Role of the lateral hypothalamus in brain states

The hypothalamus, more specifically the lateral hypothalamus (LH), is known for its key function as a homeostatic regulator, and integrator of environmental stimuli and internal signals (Fonyó, 2011; Bonnavion, et al., 2016). As these are extremely widespread and diverse functions, the structure itself must necessarily be widely connected with a plethora of other brain structures (summarized in Figure 9). However fascinating the homeostatic and behavioral

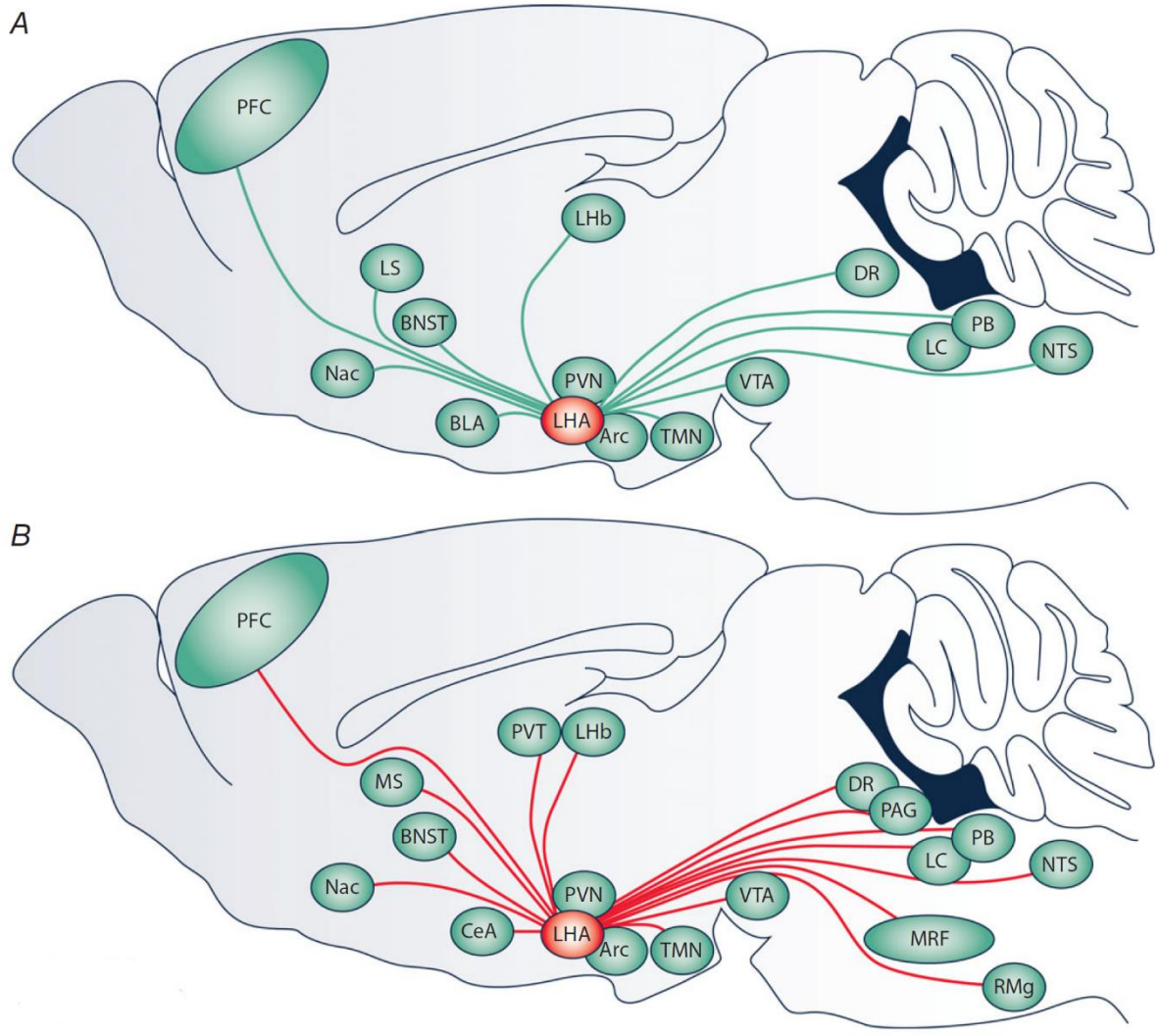

Figure 9. *Long-range connectivity of the LHA as a substrate for complex behavior*. Long-range anatomical inputs and outputs of the LHA reflect the engagement of multiple physiological systems to regulate fundamental behavioral programs. A, schematic of a parasagittal rodent brain illustrating major long-range inputs (green lines) to the LHA. B, similar schematic illustrating major long-range outputs (red lines) from the LHA. The following abbreviations are used: Arc, arcuate nucleus; BLA, basolateral amygdala; BNST, bed nucleus of the stria terminalis; CeA, central nucleus of the amygdala; DR, dorsal raphe; Fx, fornix; LC, locus coeruleus; LHA, lateral hypothalamic area; LHb, lateral habenula; LS, lateral septal nuclei; MRF, midbrain reticular formation; MT, mammillothalamic tract; NAc, nucleus accumbens; NTS, nucleus of the solitary tract; PAG, periaqueductal grey; PB, parabrachial nucleus; PFC, prefrontal cortex; PVN, paraventricular nucleus of the hypothalamus; PVT, paraventricular nucleus of the thalamus; RMg, nucleus raphe magnus; TMN, tuberomammillary nucleus; VTA, ventral tegmental area. (Bonnavion, et al., 2016)

implications of LH functioning might be, I would like to concentrate only on its projections to TRN and dorsal raphe nucleus (DRN). Not surprisingly, there have been studies that addressed its role in sleep-wake cycles and brain states (Herrera, et al., 2016; Hassani, et al., 2010). Although an indirect connection to the LGN, empirical evidence has shown that a subset of GABAergic lateral hypothalamus (LH_{GABA}) cells sends monosynaptic connections to (also GABAergic) TRN cells, and that these cells exerted a strong $GABA_A$-mediated inhibitory action on TRN cells during spontaneous NREM sleep-to-wake transitions (Herrera, et al., 2016). Optogenetic activation of the LH_{GABA}-TRN circuit promoted rapid wakefulness and cortical arousal selectively during NREM sleep and anesthetized states, respectively, as measured by a prominent change in thalamocortical oscillations (that is, sudden decrease of the amplitude of <4 Hz oscillations and burst-suppression mode, respectively) (Herrera, et al., 2016). Strikingly, the stimulation of this subset of cells was faster than optogenetic activation of norepinephrine neurons from the locus coeruleus, and the LH_{GABA}-TRN arousal circuit is specific to NREM sleep, as its activation during REM sleep did not result in any noticeable behavioral transitions (although, activation of norepinephrine-containing LC cells induce arousal both from NREM and REM sleep) (Herrera, et al., 2016).

Although DRN is most often implicated in mood regulation, it is fair to assume that it also plays a role in sleep regulation, since the main pathophysiological mechanisms involving DRN, such as depression, is frequently accompanied by sleep disturbances (Lowry, et al., 2008). Also, various waking brain states beside sleep-wake cycles can be suspected to be influenced by the DRN, as its major neuromodulator serotonin rapidly influences sensory, motor, and cognitive functions (Lottem, et al., 2016; Miyazaki, et al., 2014). The findings which describe the relationship between DRN-projecting LH axons and sleep-wake transition is elaborated in detail in the Results section of this thesis.

The Greek philosopher Heraclitus famously said, “No man ever steps in the same river twice, for it’s not the same river and he’s not the same man.” Likewise, neuroscientists are faced with ever-changing patterns of activity in the awake brain, many of which take the form of state changes. Luckily, detailed observation of these rapid state fluctuations can significantly account for variability and allow for a more accurate exploration of the neural mechanisms of behavior at all levels, from sensory coding, through decision making, to motor response. In this thesis, I would like to add my drop of detailed observations to the ocean of Neuroscience.

4. AIMS

The state dependent activity of various cortical areas has been extensively studied but this phenomenon has been less explored in subcortical areas including the thalamus. Using a combination of extra- and intracellular recordings from identified thalamic neurons, optogenetics, pharmacological inactivation and pupillometry in awake head-restrained mice our specific aims were:

I. To reveal whether and how the activity of neurons in the visual thalamus, i.e., the lateral geniculate nucleus differs between active and quiet wakefulness.

II. To elucidate the underlying cellular and network mechanisms of this state dependent activity.

III. To explore the functional implications of this brain state dependent activity, that is, how does it influence visual information processing?

IV. To test the effects of local stimulation of GABAergic axons in the DRN originating in the LH in terms of brain states.

5. MATERIALS AND METHODS

5.1. Surgical preparation

Our experiments were conducted on 17 adult male or female C57BL/6 mice which were awake, drug-free and head-restrained throughout the recording sessions. Prior to surgical preparation, the animals were anaesthetized with Isoflurane (Forane®, Abbvie, USA; dose: 1 L/min 1-1.5% isoflurane and 99-98.5% O_2) until surgical plane anesthesia was achieved, i.e., negative paw withdrawal reflex. During surgical preparation the skull of the animal was exposed by removing the skin overlying the cranium and a stainless-steel head post cemented over the frontal suture with dental pattern resin (GC America, USA). Craniotomy positions were marked with a permanent marker pen at the following stereotaxic coordinates (Paxinos and Franklin, 1997): AP: -1.9 mm; ML: 2.1 mm and DV: 1.9-3.3 mm (from dura) for LGN and AP: -4.45, ML: +1.2, DV: 2.9-3.1, at a 30° angle for DRN and AP: -2.9 mm; ML: 2.5 mm and DV: 0.3-0.6 mm For V1. At the end of the surgical procedure, the mice received 0.3 ml 1% Rimadyl (Pfizer, USA) intraperitoneally for postoperative analgesia and a 0.1 ml intramuscular injection of Gentamycin (source). 5 days after the surgical preparation the mice were handled gently each day in order to reduce excessive stress or anxiety during the recording sessions. On the day of the recording, craniotomy was performed at the previously marked stereotaxic positions under isoflurane anesthesia (Forane®, Abbvie, USA; dose: 1 L/min 1-1.5% isoflurane and 99-98.5% O_2) and mineral oil was applied on the dural surface to prevent dehydration. Finally, mice were transferred to a recording setup where their head posts were fixed to a custom clamping apparatus and recording sessions started at least 30 minutes following awakening.

5.2. In vivo electrophysiology and juxtacellular labeling

Single-unit and local field potential (LFP) recordings were performed from the LGN and V1 structures with either borosilicate glass micropipettes (Harvard Apparatus, USA) filled with 0.5 M NaCl solution containing with 1.5% w/v Biocytin (Sigma Aldrich, USA) or Silicon probes (single shank, 32-channel, Neuronexus). In the LGN, high-impedance sharp electrodes (10-80 MΩ) were used, while recordings in V1 were performed using lower resistance

electrodes (3-5 MΩ). Intracellular recordings, using the current-clamp technique, were performed with standard wall glass microelectrodes filled with 1 M potassium acetate (impedance 30-50 MΩ). When advancing the electrode through the LGN, the voltage output (V_{out}) of the amplifier has regularly (every minute) been zeroed and the bridge continuously balanced throughout the recordings. At the end of the impalement, the V_{out} was read and the recorded V_m adjusted if necessary. Recorded neurons were included in the data set only if their resting membrane potential during the active period was more hyperpolarized than -45 mV and had overshooting action potentials. A motorized micromanipulator (Scientifica, UK) and an oil hydraulic micromanipulator (Narishige, Japan) were used for advancing the microelectrodes to the LGN and V1, respectively. The dorsoventral (DV) coordinates were 2200-3000 µm for the LGN and 300-800 µm for V1. The biological signals were pre-amplified with Axon HS-9A headstages (Molecular Devices, USA) and amplified with an Axoclamp 900A amplifier (Molecular Devices, USA) (gain: 50-100x) and filtered (0.1 Hz -200 Hz for LFP, 0.3-6 kHz for units, DC-6 kHz for intracellular recordings). The amplified signals were then digitized with a CED Power3 1401 AD converter (Cambridge Electronic Design, UK) at 30 kHz sampling rate and Spike2 software (Cambridge Electronic Design, UK) was used for data acquisition.

To confirm the morphology and location of the recorded neurons as TC neurons in the LGN, we also performed juxtacellular labeling of LGN cells (n=7) by applying pulses of anodal current (1-3 nA, 500 ms, 50% duty cycle) for 2-5 minutes, which allowed Biocytin from the micropipette solution to enter the cells. At the end of the recording sessions, mice were overanesthetized, their brain removed and transferred to 4% paraformaldehyde (PFA) solution in 0.1 M phosphate buffer (PB) for overnight storage at 4°C. Next day, the brain was washed in standard PB solution and 50 µm slices containing the LGN were cut with a VT1000S vibratome (Leica, Germany). During the histological processing, the slices were cryoprotected with 10% and 20% sucrose solution, cells were opened with a freeze-thaw method and TBS-Tween20 to be able to conjugate the Biocytin in labelled cells with Cy3-Streptavidin (Jackson ImmunoResearch, USA) as secondary antibody. After 2 hours of incubation with Cy3-Streptavidin, the slices were mounted on glass microscope slides and covered with cover slips. A BX60 fluorescent microscope (Olympus, Japan) and a Surveyor software (Objective Imaging, UK) were used to visualize the labeled neurons. The identity of the labeled neurons was confirmed as LGN TC neurons according to the position of their somata and their somatodendritic morphology.

5.3. Local photostimulation of LH axons in the DRN

For in vivo optogenetic activation of LH axons in the DRN, Vgat-IRES99 Cre mice (Vong, et al., 2011) were injected with 150 nl AAV1-CAGGS-FLEX-CHR2-td tomato-SV40 bilaterally into the LH. Following 2 weeks of postinfection DRN neurons were recorded in awake head restrained mice using a multi-site Silicone electrode (Neuronexus, 32 channel, linear) coupled to an optical fiber.

5.4. Cortical inactivation with muscimol

For inactivation of the V1, we microinjected muscimol, a $GABA_A$ receptor agonist (200 nL, 1 mM), through a glass pipette (15 μm tip diameter) at coordinates 3.3 mm posterior; 2.3 mm lateral to Bregma at a depth of 0.5 mm from brain surface. The correlation of the LGN neuron baseline activity and pupil diameter was quantified and compared with control (n = 7 neurons). Saline injections (200 nl) into the V1 did not affect the correlation of LGN neuron baseline activity and pupil diameter (n = 5 neurons).

5.5. Pupillometry and visual stimulation

Pupillometry was conducted with an infrared camera (Genie^{TM}, Teledyne Dalsa, Canada) operating at 50 fps focused on the ipsilateral eye of the animal illuminated with an infrared LED (850 nm, Marubeni, Japan). For the visual evoked responses, we placed a PC screen at a ~20 cm distance to the contralateral eye of the mouse displaying moving gratings of 8 different orientations in pseudorandom order. Each grating cycle ran as the following: first it appeared and remained still for 1 s, then drifted for another second in one of the 8 orientations and eventually disappeared so only the grey screen (50% luminance) was displayed for 4 s. Afterwards the cycle restarted with a different orientation.

5.6. Data analysis

Data analysis was performed offline with custom-written MATLAB routines and ImageJ plug-ins. Recordings during stages of natural sleep (as confirmed by cortical LFP analysis) have been excluded from data analysis. Pupillometry was carried out offline on recoded AVI files using a custom ImageJ plug-in. The plug-in extends the Snakuscules model (Thevenaz & Unser, 2008) for video files. The model is designed to find circular objects using a variational framework, by minimizing an energy function. The model consists of a circle and a ring on it such that their area is always the same. In other words, the radii of the inner and outer circle always have the same ratio. The energy function is simply the difference of the intensities covered by the ring and the circle, which is minimal when the circle fits a circular (bright) object, and the ring is in the background (dark). Initially, a rectangular region in the iris is manually selected for reference pixel intensities, which are then used to invert the image such that this region is dark and the pupil white. Afterwards, the user must provide the segmentation manually in the first frame of the video. Assuming that the change between two consecutive frames is small (due to the 50-fps camera used), the software uses the segmentation of the previous frame as an initial solution for the subsequent frame. The results are then written to a CSV file, including the frame index, pupil position, and radius. Black frames that are used for synchronization of the video files and electrophysiology are also detected and indicated in the result file. Segmentation is not performed in black frames.

For comparing the FRs of thalamic neurons with respect to the pupil diameter, the upper and lower terciles of the pupil diameter distributions were used. LGN neurons were identified as TC or interneurons based on either their morphology (n = 7 TC neurons labeled), action potential duration (<0.35 ms for LGN interneurons, >0.35 ms for TC neurons, see Fig. 16 A), and action potential height ratio (Fig. 16 A, left). A burst in thalamic neurons was defined as a cluster of spikes consisting of minimum of two action potentials, a maximum interspike interval of 10 ms, and had to be separated from other bursts by more than 100 ms. Brain states were detected from the V1 LFP signal using a semi-automated level threshold method in Spike2 (CED, UK). Quiet wakefulness (QW) states were defined as periods of at least 3 s with large amplitude (2×baseline) 3–6Hz voltage fluctuations. The timing of state changes was determined by detecting the peak of the first 3–6 Hz oscillation cycle for active wakefulness (AW) to QW transitions and of the last peak of the 3–6 Hz oscillation cycle for QW-to-AW transitions. Periods of dilated pupil correspond to the upper tercile and periods of constricted pupil to the

lower tercile of the pupil distribution for a given recording. For correlating pupil diameter and FRs, we used the random permutation test, in which two data points were randomly selected and paired up from the FR and pupil data points (i.e., one from each), and this was repeated 1000 times, resulting in a (normal) distribution of random data pairs serving as null hypothesis, and two-tailed *P*-values were calculated. Pearson's *r* calculated from the real (observed) FR/pupil diameter data was then compared to the random distribution, and *r* values falling out of 95% confidence intervals were considered statistically significant.

Visual evoked responses were determined by comparing the firing rate during three periods of time: (1) 1 s before the appearance of the grating image, (2) 1 s during still image presentation and (3) 1 s of drifting grating. We used Wilcoxon rank-sum test to determine two p-values (P1 and P2). P1 is from comparing the firing rates of (1) and (2), and P2 is from comparing (1) and (3). Significant evoked responses were determined when P2 was statistically significant ($p<0.05$) and P1 was not ($p>0.05$), thus excluding potentials evoked merely by illumination change of the PC screen. After compiling firing rate changes in all 8 different orientations, Orientation Selectivity Index (OSI) was calculated with the following formula:

$$OSI = \frac{preferred\ orientation - orthogonal\ orientation}{preferred\ orientation + orthogonal\ orientation}$$

where orthogonal orientation was calculated as the mean of preferred orientation + and – 90°. Several time frames were omitted from analysis when the mouse blinked, and the missing data points were replaced by linear interpolation. Pearson correlation coefficients (R) regarding spontaneous brain state dependent activity and statistical significance defined by random permutation test calculated using MATLAB.

6. RESULTS

As most of the recent findings concerning the mechanisms and effects of brain states focus on neocortical areas, we aimed to address the aforementioned phenomena in the LGN of awake mice, which is known to be the thalamic relay nucleus involved in visual signal processing (Motokawa & Suzuki, 1966).

Visual information reaches the V1 via the LGN (Murphy, et al., 1999). Consequently, the first level of integration on which visual information is processed takes place in the LGN and that is the very reason we endeavored to investigate the activity of TC cells in this nucleus. According to numerous previous studies, TC cells classically exhibit two modes of firing: (1) burst firing during states of hyperpolarized membrane potential states and (2) tonic firing mode when the membrane potential of TC cells is depolarized (Jahnsen & Llinas, 1984; Jahnsen & Llinas, 1984; Hirsch, et al., 1983; McCormick & Bal, 1997; Hughes, et al., 2002; Hughes, et al., 2004; Lőrincz, et al., 2009b; Crunelli, et al., 2012). However, the novel view is that there is a third mode of firing: a subset of TC cells can generate burst activity at depolarized membrane potential states, called high-threshold (HT) bursts (Hughes, et al., 2002; Crunelli, et al., 2012). Our findings suggest that these firing patterns transiently alternate in relation to state transitions in awake, drug-free and spontaneously active brains of mice. Moreover, we wanted to explore the origin of this relationship by the inactivation of corticothalamic input to the LGN (Wilson, et al., 1984) using muscimol applied to the V1.

We also addressed the brain state dependent performance alterations of the visual sensory pathway by eliciting orientation selective visual responses in the LGN during various states. While apparent visual responses were evoked in the LGN TC cells, we obtained a somewhat counterintuitive result, namely the orientation selectivity decreased during locomotion and alert wakefulness compared to stationary behavior and relaxed brain states. These findings might have important implications on thalamic visual sensory processing.

Although sensory information processing and brain state dependency is mainly studied in the thalamocortical circuitry, several other subcortical areas are known to be involved global state transitions, e.g., from sleep to wake, including the LH and the DRN (Hassani, et al., 2010; Herrera, et al., 2016), thus we conducted in vivo experiments to explore the role of LH-DRN circuit in promoting wakefulness.

6.1. The spontaneous activity of LGN is correlated with arousal

Extracellular and intracellular recordings of morphologically identified LGN neurons with simultaneous LFP in the V1 and pupillometry in awake head-restrained mice revealed the brain state-dependent activity of thalamic neurons in the LGN. The pupil diameter of awake mice

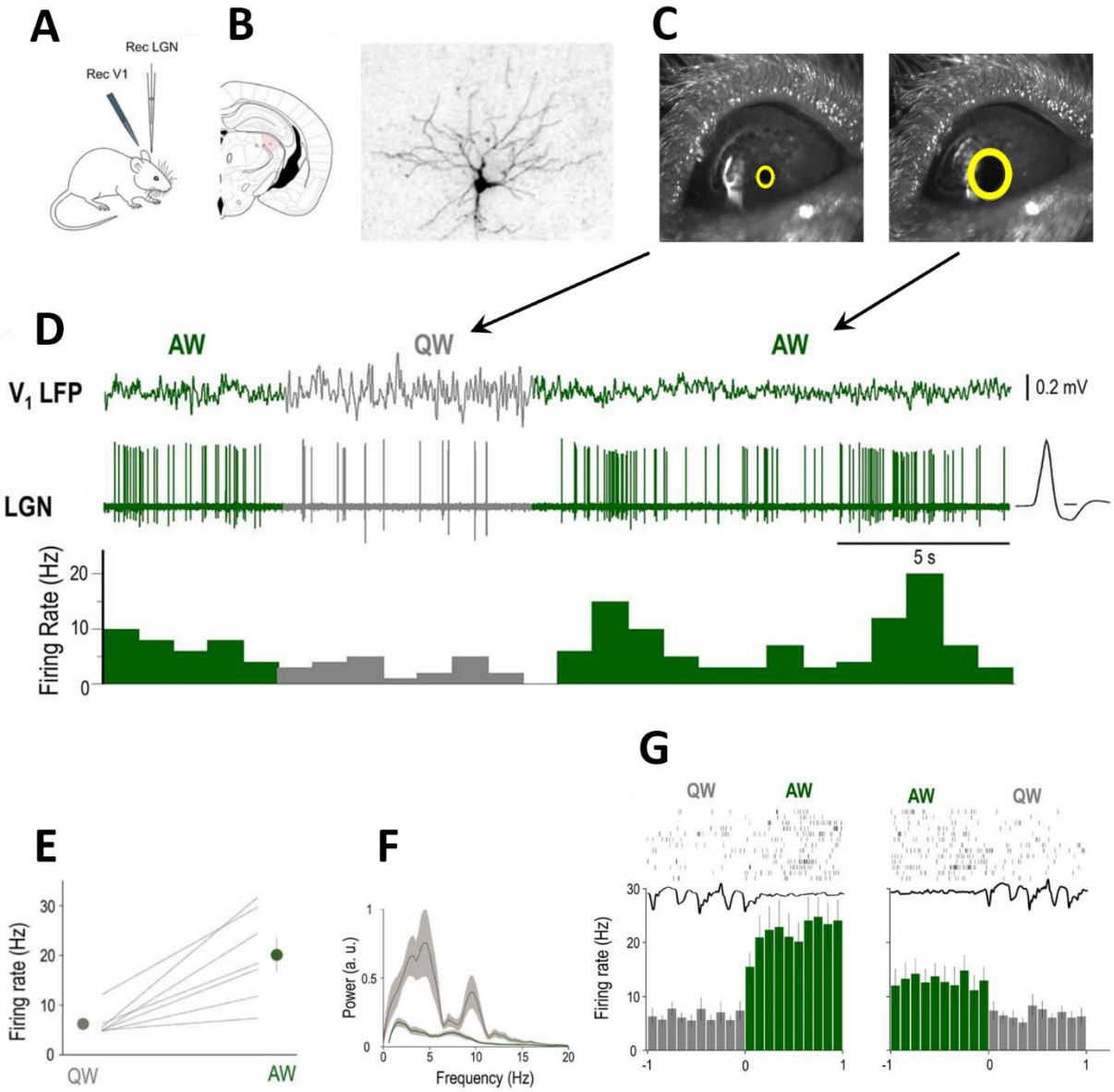

Figure 10. *The baseline firing of identified LGN neurons is brain state dependent.* (A) Schematics of the experimental setup. (B) Coronal brain section shows the location (left) and morphology (right) of a neuron recorded and labeled in the LGN. (C) Examples of constricted and dilated pupils recorded by video camera. Note the arrows pointing to corresponding cortical states. (D) Example of simultaneous V1 LFP and unit recording from the LGN neuron shown in B in an awake head-restrained mouse. Spontaneous state transitions are color coded for clarity (AW: green; QW: gray). Averaged action potential waveform is shown on the right, calibration: 0.2 ms. (E) Mean FR changes between QW and AW for all identified LGN TC neurons (n=7). (F) Power spectrum of the QW and AW states for all the recordings from morphologically identified TC neurons (n=7) Note the peaks in power at theta (3-5 Hz) and alpha (8-13 Hz) frequencies. (G) Schematic state transition raster plot of the LGN neuron (top), V1 LFP (middle), and peri-event histogram (bottom); state transitions color coded as in D. Modified from Molnár et al 2021.

spontaneously fluctuated during the recordings, with states of quiet wakefulness (QW) associated with constricted pupil and periods of active wakefulness accompanied (AW) by pupil dilation. States of QW were characterized by large-amplitude slow V1 LFP fluctuations (mean peak-to-peak amplitude 0.77±0.2 mV, $n = 98$), and small pupil diameter, while periods of active wakefulness (AW) by small-amplitude fast fluctuations (mean peak-to-peak amplitude 0.27±0.11 mV, $n = 98$) in the LFP recorded in V1 with prominent pupil dilation (Fig. 10 C and D). State transitions were accompanied by prominent changes in the activity of LGN neurons as well (Fig. 10 D). Consistently enough, QW to AW transitions led to an increase in firing (Fig. 10 D and E), and AW to QW transitions led to a decrease in firing (Fig. 10 D) in the majority of LGN neurons. These neurons were classified as TC neurons by either morphology (Fig. 10 B, n = 7) or electrophysiological properties (see details later). The increased firing rate

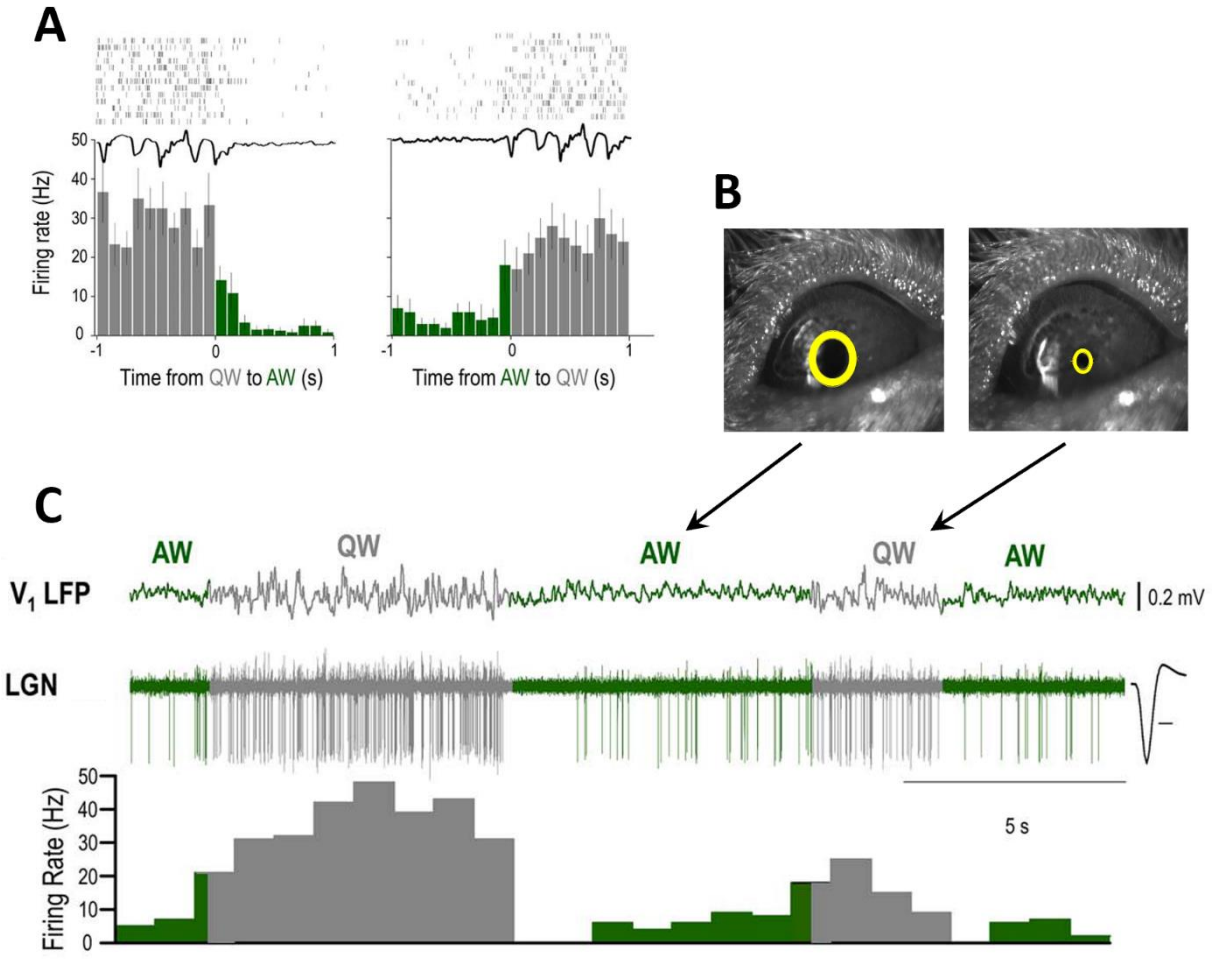

Figure 11. *The activity of a subset of LGN neurons appears to be the inverse of TC cells.* (A) Schematic state transition raster plot of the LGN putative interneuron (top), V1 LFP (middle), and peri-event histogram (bottom). Spontaneous state transitions are color coded for clarity (AW: green; QW: gray). (B) Examples of constricted and dilated pupils recorded by video camera. Note the arrows pointing to corresponding cortical states. (C) Example of simultaneous V1 LFP and unit recording from a putative LGN interneuron in an awake head-restrained mouse. State transitions color coded as in A. Note the high baseline FR during QW. Averaged action potential waveform is shown on the right, calibration: 0.2 ms. Modified from Molnár et al 2021.

in the majority of LGN cells was associated with cortical desynchronization in V1 and pupil dilation (Fig. 10), while the marked drop in neuronal activity when pupil diameter decreased indicated relaxed wakefulness with synchronized activity in the neocortex and the replacement of high frequency brain waves with slower oscillations. Strikingly, a subset of LGN neurons characterized by high baseline FR (Fig. 11) also showed state transition-related changes of baseline activity. In this neuronal subset, QW to AW transitions led to a decrease in firing rate (Fig. 11 A and C), but AW to QW transitions resulted in an increase in firing (Fig. 11 A and C), leading to the suspicion of them being local interneurons.

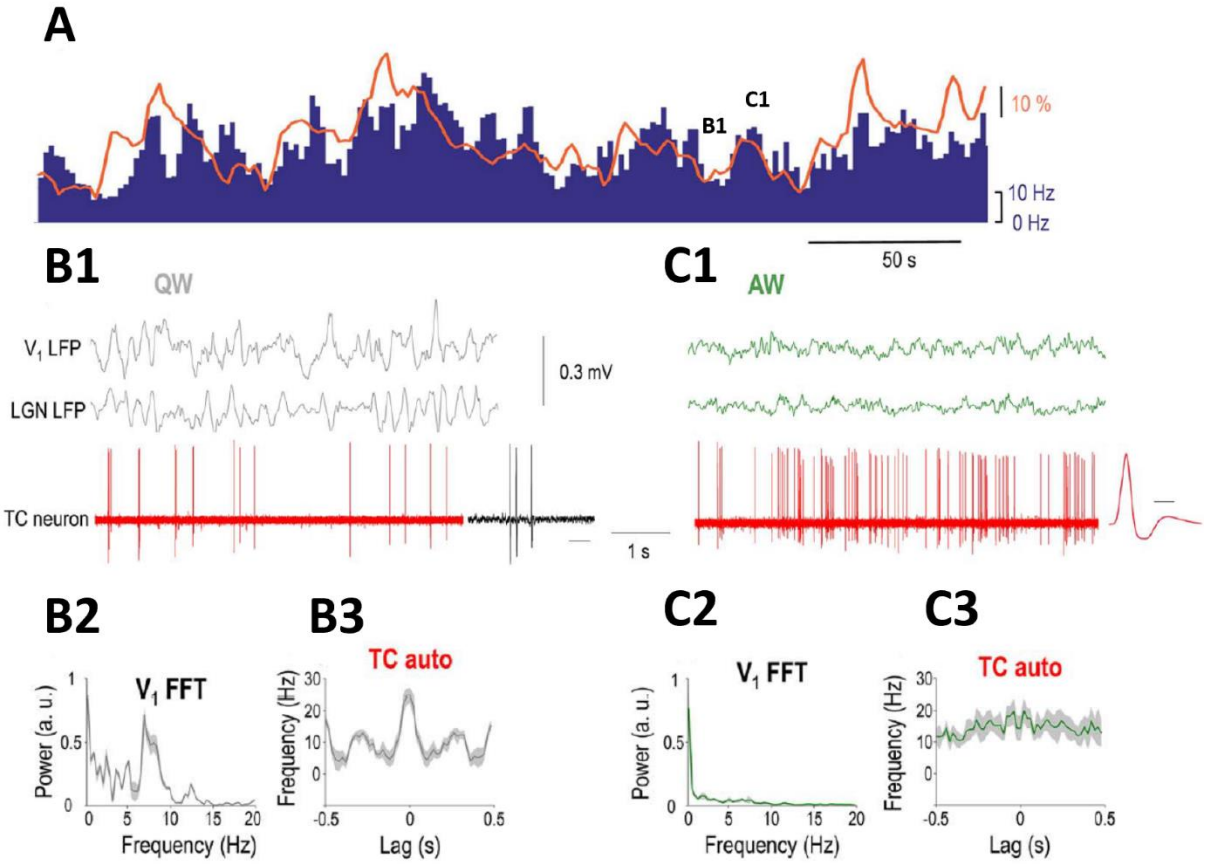

Figure 12. *LGN TC neurons are positively correlated with arousal.* (A) FR of the LGN TC neuron (blue bars) increases when the simultaneously recorded pupil (orange line) is dilated but decreases when the pupil is constricted. (B1) Simultaneously recorded V1 LFP, thalamic LFP, and single units of the TC neuron shown in A shown on a faster time-base during a period of constricted pupil (marked in A as B1) corresponding to a state of QW. Note the presence of putative LTS-mediated bursts enlarged on the right (calibration: 50ms). (B2) V1 power spectrum, (B3) autocorrelation of the TC neuron shown in A. (C1) Simultaneously recorded V1, thalamic LFP, and single units of the TC neuron shown in A plotted on a faster timescale during a period of dilated pupil (marked on A as C1) corresponding to a state of AW. The average action potential waveform is shown on the right (time calibration: 0.5 ms). (C2) V1 power spectrum, (C3) autocorrelation of the TC neuron shown in A. Modified from Molnár et al 2021.

To further drill down in the mechanism of state dependent activity of LGN neurons, we quantified the correlation between neuronal firing rates (FR) and pupil diameter and found three functionally distinct groups of cells: non-modulated, positively correlated (regarded as TC neurons), negatively correlated (regarded as putative interneurons) cells. A smaller percentage

of neurons (n = 25/98, 26%) had a baseline activity that did not correlate with the pupil diameter (P > 0.05, random permutation test), while the majority did (n = 73/98, 74%). In most of the state-modulated neurons, FRs showed a statistically significant positive correlation with pupil diameter (57 of 73 significant cells P<0.05, random permutation test; mean Pearson's r = 0.411±0.025 Hz, Fig. 12). Both neuron groups were classified as TC neurons either morphologically (n = 7) or using physiological criteria, as follows. The duration of the action potentials was relatively large (positively modulated: 0.43±0.01 ms, non-modulated: 0.48±0.02 ms) and homogeneous (the action potential durations were not significantly different in the two groups, P > 0.05, Wilcoxon rank-sum test) in both groups. Figure 12 illustrates an example morphologically identified LGN TC neuron showing a positive correlation with pupil diameter. Note that the periods of constricted pupil coincide with QW states and putative low-threshold spike (LTS) mediated burst firing of the LGN TC neuron (Fig. 12 B1), whereas the periods of dilated pupil with AW states and high-frequency tonic action potential output (Fig. 12 C1). Additionally, periods of pupil constriction correspond to QW states as the V1 LFP shows a clear peak in the 3–5 Hz band (Figs 12 B1 and B2) and the autocorrelation of the TC neuron low-frequency rhythmic burst firing (Fig. 12 B3). Conversely, periods of pupil dilation correspond to AW states as the V1 LFP shows no peak in the 3–5 Hz band (Fig. 12 C2) and the autocorrelation of the TC neuron reveals high-frequency tonic firing (Fig. 12 C3).

Perhaps the most astounding finding was that we recorded a subset of neurons showing negative correlation to pupil diameter (16/98, 16% of all recorded cells, P<0.05, random permutation test; mean Pearson's r =-0.4±0.045). The duration of the action potentials in these neurons was significantly narrower than in TC neurons (0.23±0.01 ms in negatively correlated neurons vs. 0.44±0.01 in putative TC neurons, P<0.05, Wilcoxon rank-sum test), and the waveform of their action potential was more biphasic (height ratio: 0.41±0.02 in putative TC neurons, 0.73±0.04 in negatively correlated neurons, P<0.05, Wilcoxon rank-sum test) (Figs 13 B1 and C1). These neurons were classified as putative LGN interneurons. Figure 13 illustrates an example putative LGN interneuron showing a negative correlation with pupil diameter. Note that during the periods of constricted pupil characteristic of QW states (Fig. 13 B1) this putative LGN interneuron is more active than during AW (Fig. 13 C1). Also note that the activity of the putative LGN interneuron consists of tonic action potential output during both QW (Fig. 13 B3) and AW (Fig. 13 C3).

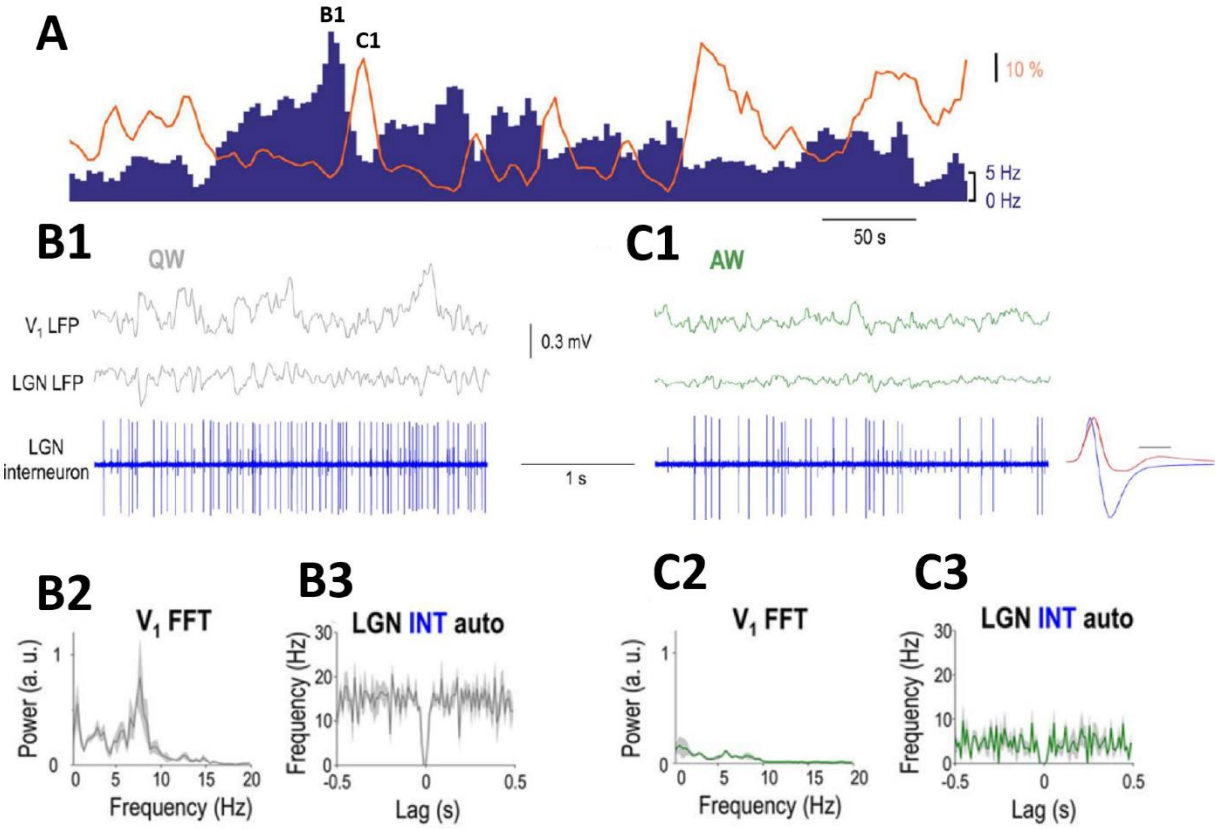

Figure 13. *A subset of LGN interneurons is negatively correlated to arousal.* (A) FR of an example LGN interneuron (blue bars) decreases when the simultaneously recorded pupil (orange line) is dilated but increases when the pupil is constricted. (B1) Simultaneously recorded visual cortical, thalamic LFP, and single units of the LGN interneuron shown in A plotted on a faster time-base during a period of constricted pupil (marked in A as B1) corresponding to a state of QW. (B2) V1 power spectrum, (B3) autocorrelation of the putative LGN interneuron shown in A during 10 consecutive periods of constricted pupil. (C1) Simultaneously recorded V1, thalamic LFP, and single units of the putative LGN interneuron shown in A plotted on a faster time-base during a period of constricted pupil (marked in A as C1) corresponding to a state of AW. The average action potential waveform is shown in the right (blue, time calibration: 0.5 ms) with the average action potential of the TC neuron (red) from Figure 12 overlaid for comparison. Note the presence of a second neuron (smaller spikes) not correlated with the pupil diameter. (C2) V1 power spectrum, (C3) autocorrelation of the LGN interneuron shown in A during 10 consecutive periods of dilated pupil. Modified from Molnár et al 2021.

6.2. The membrane potential of LGN TC neurons is correlated with brain states

To elucidate the intracellular mechanisms underlying the state-dependent fluctuation of thalamic neurons, we performed intracellular recordings of LGN TC neurons (n=5) of awake mice while simultaneously monitoring the pupil diameter (n=4) and recorded the LFP and multi-unit activity (MUA) in V1 (Fig. 14). In all the neurons recorded, we found an apparent correlation between the membrane potential and pupil diameter (Fig. 14 B), such that periods of pupil constriction were associated with low baseline FRs (6.98±3.19 Hz), hyperpolarized

membrane potentials (−63.0±2.3 mV) and burst firing in two of the neurons recorded (Fig. 14 A bottom right). Importantly, these bursts were recorded at a membrane potential inconsistent with LTS and more akin to HT burst (Lőrincz, et al., 2009b; Crunelli, et al., 2012; Crunelli, et al., 2018) (Fig. 14 G). In addition, the interspike interval of the first and second action potentials in LTS and HT bursts was different (LTS: 3.38±0.15 ms, HTB: 8.15±2.69 ms, $P<0.001$, Wilcoxon rank-sum test, Fig. 14 I) corroborating the idea that they represent high-threshold bursts (Hughes, et al., 2004; Lőrincz, et al., 2008; Lőrincz, et al., 2009b; Crunelli, et al., 2012). Periods of pupil dilation, on the other hand, were associated with high frequency (19.96±10.98 Hz, Fig. 14 A) tonic action potential output and less hyperpolarized membrane potentials (−59.1±2.82 mV, Fig. 14 A left). When quantifying the correlation of the low-pass filtered membrane potential and pupil diameter, we found that the membrane potential of LGN TC neurons was lagging the changes in pupil diameter by approximately 5 s (Fig. 14 D). Large amplitude retinogeniculate EPSPs were not state dependent (mean EPSP rate QW:

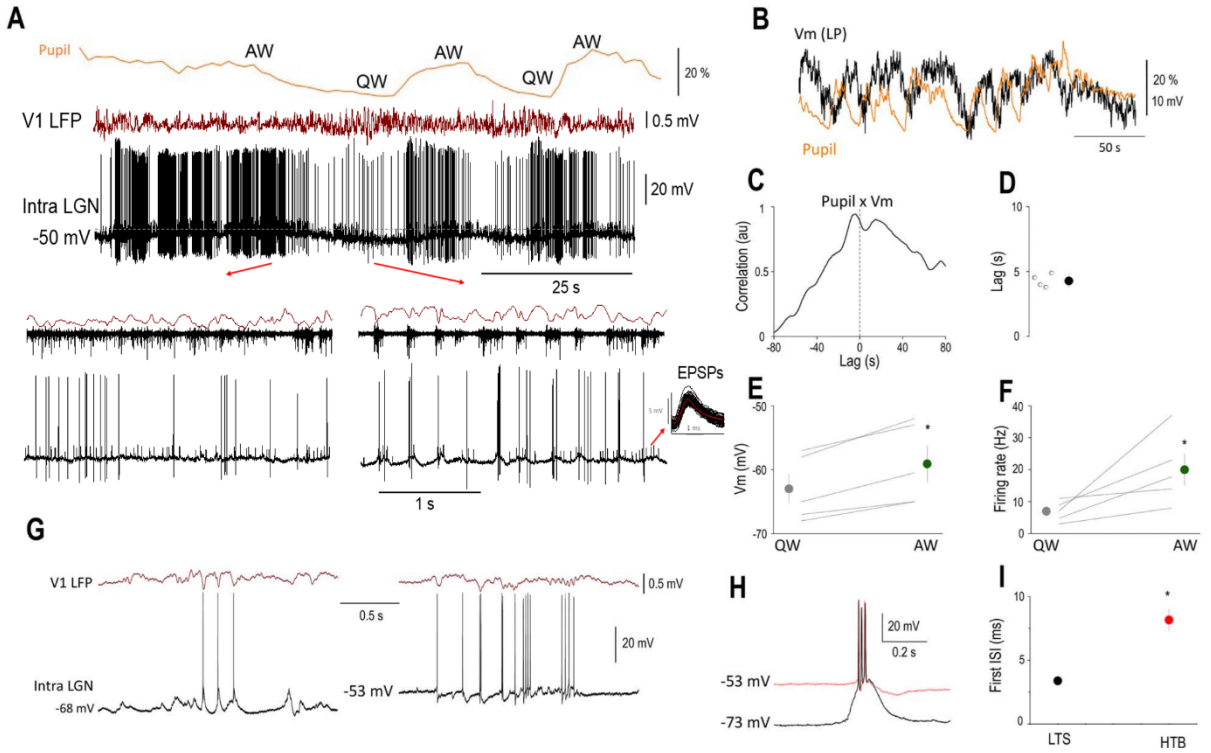

Figure 14. *The membrane potential of LGN TC neurons is correlated with brain states.* (A) Simultaneous pupillometry (top), cortical LFP (middle), and LGN Vm recording (bottom) during state transitions in an awake head-restrained mouse. Quiet wake (QW) and active wake (AW) states are indicated by red arrows and shown on a faster time-base below the Vm recording; top trace: V1 LFP, middle: V1 MUA, bottom: Vm. Note the large retinogeniculate EPSPs on the Vm recording (indicated by red arrow). (B) Slow rhythmic fluctuations in the pupil diameter are correlated with the Vm of this LGN neuron as apparent on the low-pass filtered Vm (Vm LP) overlaid on the pupillometry trace. (C) Normalized cross-correlation and (D) quantification of Vm delay in respect to pupil diameter. Mean FRs (E) and Vm (F) for the two brain states. (G) LTS and HT bursting are present in the same LGN TC neuron during QW states. During periods of relatively hyperpolarized membrane potentials (left), LTS-mediated bursts accompany V1 LFP 3–6 Hz oscillations, but HT bursts are present at less hyperpolarized membrane potentials (right). (H) Overlaid LTS (black trace) and HT bursts (red trace) recorded from the neuron in (G). (I) Mean duration of the first ISI from LTS and HT bursts, color codes as in H; ISI: interspike interval. Modified from Molnár et al 2021.

17.75±3.88 Hz, AW: 19.35±4.36 Hz, *P*>0.05, Wilcoxon's signed-rank test). Thus, the state-dependent action potential output of thalamic neurons can be accounted for by slow changes in their neuronal membrane potential.

6.3. Visually evoked responses of LGN TC cells

Next, we asked whether the visual responses elicited in TC cells are state dependent. 31 of 98 recorded LGN neurons (32%) were evaluated, as they elicited significant visual responses defined as statistically significant increase in firing rate compared to baseline activity (Wilcoxon rank-sum test, p>0.05). Analysis of the visual responses and calculating the orientation selectivity index (OSI) values revealed a slight alteration of orientation selectivity in a brain state dependent manner. Strikingly, we observed a counterintuitive change in orientation selectivity, namely in the states when the normalized pupil size was greater than 0.5

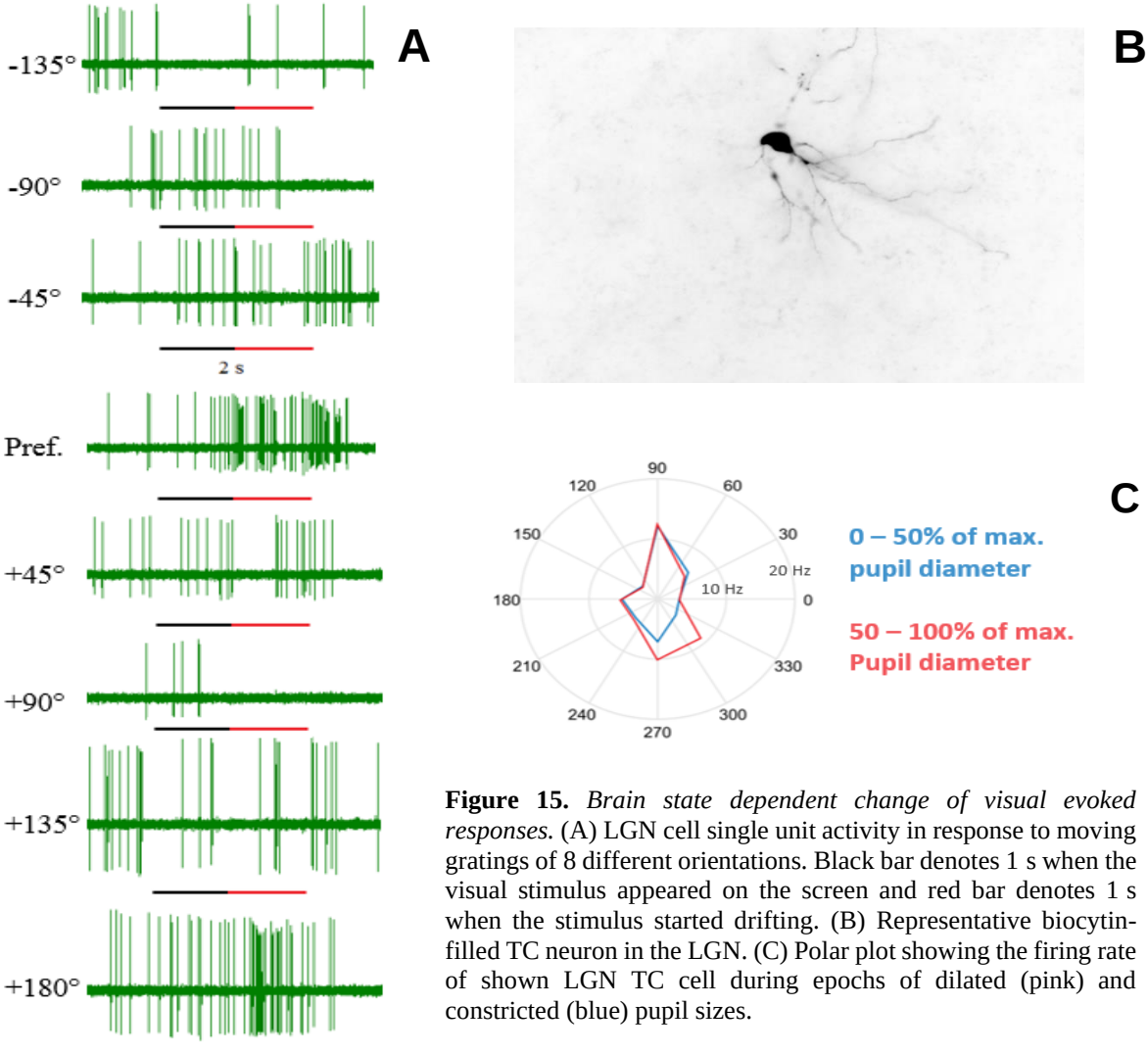

Figure 15. *Brain state dependent change of visual evoked responses.* (A) LGN cell single unit activity in response to moving gratings of 8 different orientations. Black bar denotes 1 s when the visual stimulus appeared on the screen and red bar denotes 1 s when the stimulus started drifting. (B) Representative biocytin-filled TC neuron in the LGN. (C) Polar plot showing the firing rate of shown LGN TC cell during epochs of dilated (pink) and constricted (blue) pupil sizes.

(regarded as AW), more orientations evoked significant responses in TC cells (i.e. the OSI value decreased) than in the state when normalized pupil size was smaller than 0.5 (regarded as QW) (Fig. 15).

6.4. Population-level analysis of LGN neurons

Altogether, 73 of 98 (74.5% of all) recorded LGN cells showed statistically significant brain state modulation and 57 (78.1% of significant cells) of which were positively correlated with pupil diameter and only 16 neurons (21.9% of significant cells) were negatively correlated, while the rest of the cells (n=25; 25.5% of all) showed no significant correlation to brain states (i.e., pupil size) (Fig. 16). The recorded cells were classified into three functionally distinct

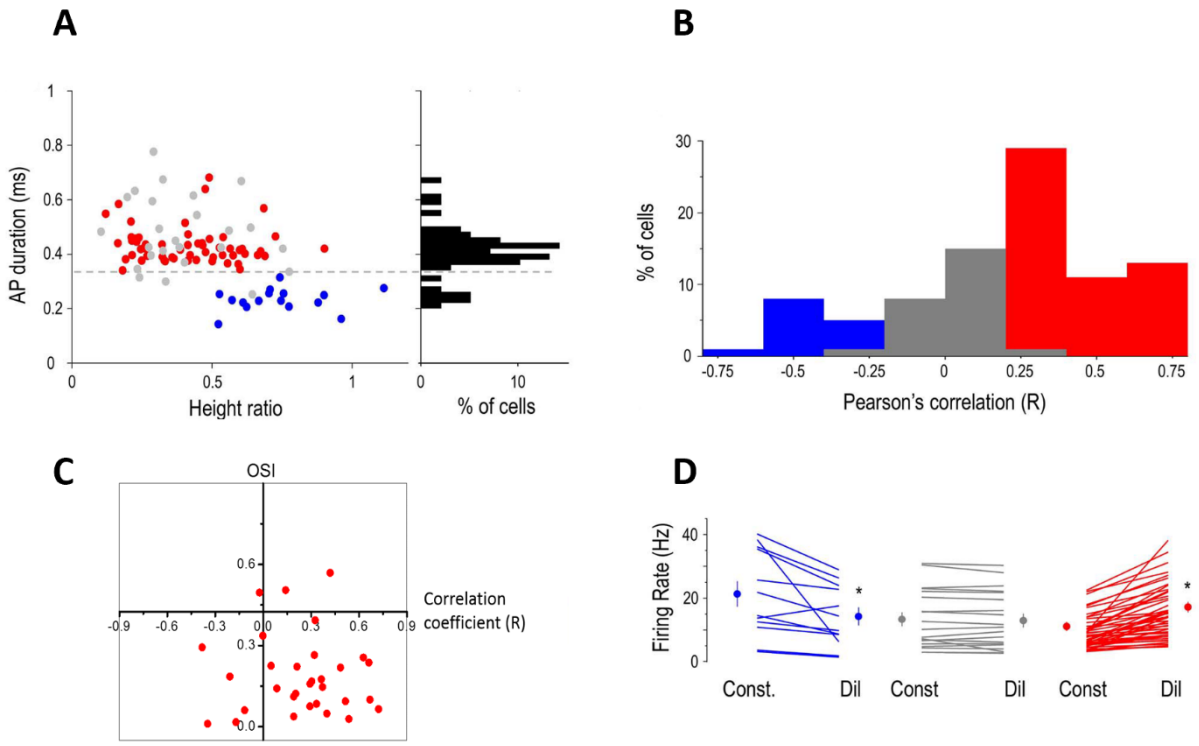

Figure 16. *Arousal-dependent activity in the LGN depends on neuronal identity.* (A) Classification of neurons based on spike waveform parameters. Scatter plot of duration versus height ratios for recorded LGN units (red: neurons positively correlated with pupil diameter, gray: uncorrelated neurons, blue: neurons negatively correlated with pupil diameter). The histogram of the action potential durations is shown on the right. Putative LGN interneurons are seen for durations <0.35 ms and putative TC neurons for durations>0.35 ms. (B) Distribution of pupil diameter/FR correlations. Putative LGN interneurons were negatively correlated (left, blue bars) and TC neurons were either uncorrelated (middle, gray bars) or positively correlated (right, red bars). (C) Scatter plot showing that correlation tends to be inversely proportional to OSI. Red dots mark individual cells (n=31). Note that the lower right corner contains the most data points where correlation coefficient is high and OSI value is low. (D) Mean FRs of individual neurons during periods of constricted (Const) and dilated (Dil) pupil. Group averages are shown on the side of each group for the two states, color codes same as in A. Panels A, B and D modified from Molnár et al 2021.

groups by their FR output (Fig. 16 A left) and action potential (AP) characteristics (Figs. 16 A right). We found only 31 of 98 (32%) state modulated cell to be visually responsive, but 15 of them (48%) showed state dependent orientation selectivity change, that is, the cell had different preferred orientation in AW than in QW (each of the two states were evaluated with Wilcoxon rank-sum test; $P<0.5$). In addition, an apparent tendency indicates that a link might exist between correlation of spontaneous firing with pupil diameter and orientation selectivity of LGN cells, i.e., neurons with activity strongly correlated with brain states have lower OSI (Fig. 16 C). These results might have important implications on brain state dependent visual sensory processing.

6.5. Corticothalamic modulation is hindered by visual cortex inactivation

As already shown, rhythmic synchronous EEG activities are correlated to LGN firing (Lőrincz, et al., 2009b), we reasoned that corticothalamic projections are, at least in part, responsible for regulating LGN activity, thus we monitored the effects of inactivating the cortical feedback from V1 to the LGN with muscimol microinjections (see Material and Methods for details) and

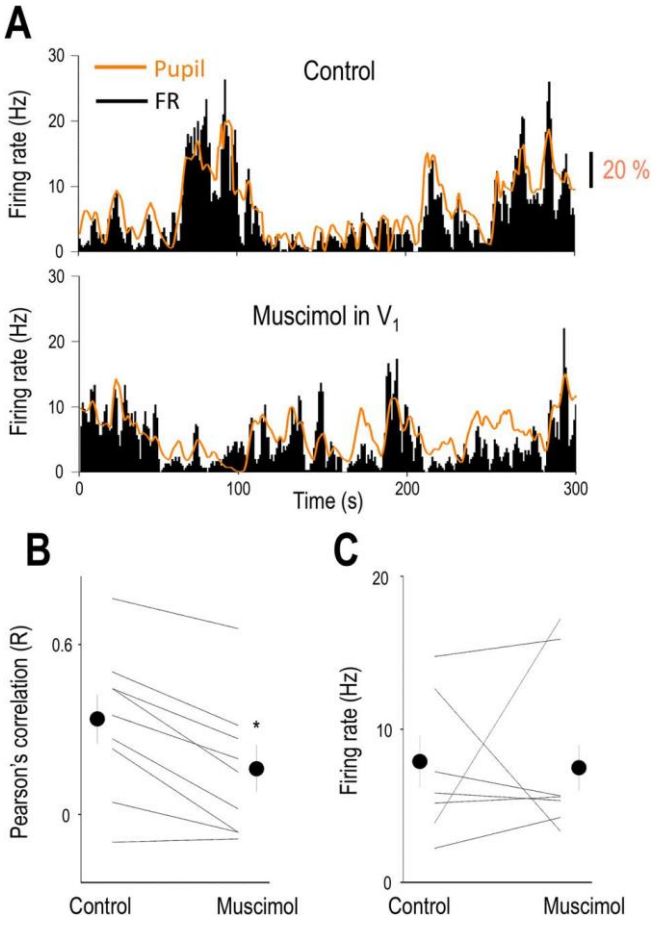

Figure 17. *V1 inactivation decreases the correlation of LGN neuron firing and pupil diameter.* (A) Baseline activity of an example thalamic neuron and the simultaneously recorded pupil diameter before (control) and following V1 inactivation. Note the spontaneous fluctuations in pupil diameter and thalamic firing in both conditions. (B) Correlation between the pupil diameter and thalamic baseline activity before (Control) and following muscimol infusion in V1. (C) Firing rate of thalamic neurons before (Control) and following muscimol infusion in V1. Modified from Molnár et al 2021.

its effect on the arousal-dependent activity of LGN neurons. Figure 17 shows the baseline activity of an example thalamic neuron and the simultaneously recorded pupil diameter. In the control condition (Fig. 17 A, top), the FR and pupil diameter changes are relatively simultaneous but following V1 inactivation periods of dilated pupil are not always followed by an increase in FR and FR changes do not always coincide with a change in pupil diameter. To quantify the relationship between pupil diameter and thalamic baseline firing in the two conditions, we compared the FR of thalamic neurons and calculated he correlation between FR and pupil diameter before and following V1 inactivation. The FR of individual neurons before and after V1 inactivation varied considerably (Fig. 17 B) but did not reach statistical significance as a group (control: 7.93±1.69 Hz, V1 inactivation: 7.52±1.47 Hz, P>0.05, Wilcoxon's signed-rank test, n = 9; Fig. 17 C). When comparing the correlation of thalamic single units and pupil diameter before and following V1 inactivation (Fig. 17 B and C), we found a significant decrease (control: 0.28±0.07, V1 inactivation: 0.13±0.06, $P<0.05$, Wilcoxon's signed-rank test, n = 9), suggesting that corticothalamic input from V1 is at least partly responsible for the state-dependent activity in LGN TC neurons.

6.6. Lateral hypothalamus axons inhibit GABAergic DRN neurons

As the neuromodulatory tone has a profound role in shaping brain states, we explored the interaction between two other subcortical areas, the LH and the DRN, the latter of which is known to be the main source of serotonin in the brain. LH GABAergic neurons have been shown to influence brain states by inhibiting the GABAergic neurons of the thalamic reticular nucleus (Herrera, et al., 2016), but whether and how LH neurons affect neuromodulation in general and DRN neurons has not yet been tested. Data from the literature shows that serotonin exerts a primarily inhibitory action on thalamic nuclei through two mechanisms: direct postsynaptic action mediated by the 5-HT_{1A} receptor and an indirect increase in IPSPs, apparently through the excitation of local GABAergic interneurons (Monckton & McCormick, 2002). Interestingly, hyperpolarizing responses to serotonin were not observed in LGN thalamocortical cells and only rarely observed in the medial geniculate nucleus, instead in these nuclei, the application of serotonin often elicited a small depolarization and increase in apparent input conductance (Monckton & McCormick, 2002), which had been shown previously to result from an enhancement of the hyperpolarization-activated cation current I_h (McCormick & Pape, 1990). To test for functional connections from LH_{GABA} projections to DRN neurons in

particular, we recorded extracellular single unit activity from DRN neurons of awake, head-restrained VGAT-cre mice infected with AAV1-CAGGS-336 FLEX-CHR2-tdTOM-SV40 in the LH while photo-stimulating ChR2-expressing LH_{GABA} axons in the DRN (5 light pulses of 10 ms at 20 Hz, 5 mW; Fig. 18). Comparison of the activity of DRN neurons recorded in the presence and absence of LH_{GABA} axonal photostimulation (5 light flashes of 10 ms at 20 Hz, 5 mW) confirmed the suppressive effect in a subset of DRN neurons (2/23, 9%), while the activity of the remaining neurons was increased (21/23, 91%). The overall activity of DRN neurons was slowly (~200 ms), but persistently (~1 sec) increased (baseline firing: 7.67±6.87 Hz, baseline firing after photostimulation: 10.98±8.920 Hz, n=12, $p < 0.001$, Wilcoxon's signed rank test, Fig. 18B).

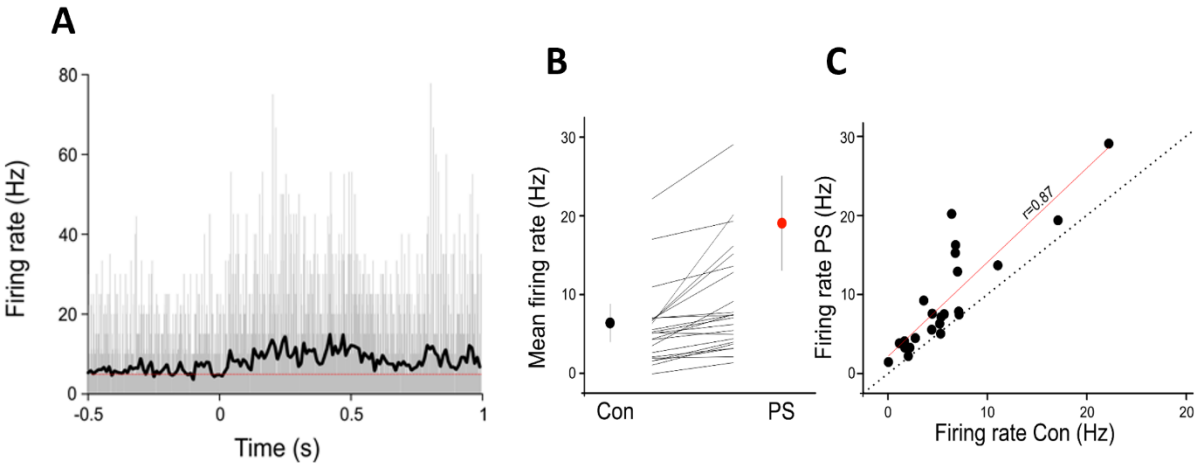

Figure 18. *Effects of LH axonal photostimulation in the DRN.* (A) PSTH of all recorded DRN neurons (n=23) aligned on the photostimulation of LH GABAergic axons in the DRN. Light gray: individual cells, black line: mean PSTH of all recorded neurons. Red dotted line: baseline firing rate. (B) Mean firing rate during control and photostimulated epochs, lines: individual neurons, black circle: control, red circle: photostimulated mean firing rate of all neurons. (C) Scatter plot of control and photostimulated mean firing rate of all DRN neurons. Dotted line: diagonal, red line: linear fit.

7. DISCUSSION

While cortical function in general and visual cortical activity in particular are well known to be modulated by the level of arousal in awake animals (McGinley, et al., 2015; Vinck, et al., 2015), the arousal-dependent activity of reciprocally connected visual thalamus is more controversial. In my dissertation, whilst exploring the answer to the questions stated in Aims, I found in awake behaving mice, that 1) the baseline LGN neuronal activity correlates with arousal during the awake state; 2) the polarity of this correlation is cell type specific, with LGN TC neurons being positively, and putative LGN interneurons negatively correlated with arousal; 3) this state-dependent activity at least partly originates from cortical feedback; 4) visual sensory processing is somewhat altered in different brain states; and 5) LH_{GABA} projections profoundly influence the activity of most DRN neurons leading to arousal from NREM, but not REM sleep (Gazea, et al., 2021). LGN activity has long been known to differ during wakefulness compared to sleep (Hirsch, et al., 1983), during alert and inattentive states (Bezdudnaya, et al., 2006), with a subset of bursting LGN TC neurons playing an important role in generating, while putative LGN interneurons in providing tonic firing TC neurons with temporally precise phasic inhibition during individual cycles of the alpha rhythm (Lőrincz, et al., 2009b). Previous results suggested that LGN spontaneous and visually evoked FRs are not different between immobile and running mice (Aydın, et al., 2018), whereas V1 activity was markedly different between the two states (Niell & Stryker, 2010). This controversy might arise from differences in the definition of brain states: whereas locomotion is only associated with alert wakefulness, both quiet and alert wakefulness can occur during immobility (Vinck, et al., 2015). Pupil diameter is an excellent proxy for a general neuromodulatory tone and brain states (Reimer, et al., 2016), and its combination with V1 LFP level of synchronization as used in the present study provides a more accurate state definition. Thus, the precise definition of brain states based on both V1 LFPs and pupillometry enabled us to reveal the state dependent activity in the majority of LGN neurons.

Our results reveal an arousal-dependent spontaneous activity in the majority of LGN neurons of awake behaving animals. Notably, the polarity of the correlation between neuronal activity and arousal, quantified by monitoring the pupil diameter, depends on neuronal identity within the LGN. Specifically, whereas TC neurons, the dominant cell type in the LGN, tend to increase their activity during AW (desynchronized V1 LFP and dilated pupil), putative LGN interneurons, which are key for intimately controlling the timing of TC neuron firing in awake

animals (Lőrincz, et al., 2009b), behave in an opposite manner showing decreased activity during AW and increased activity during QW (synchronized V1 LFP and constricted pupil). Taken together, the increase in firing in most TC neurons during AW is accompanied by a decrease in inhibition derived from local interneurons (Lőrincz, et al., 2009b). This may have implications for both the spontaneous activity of LGN TC neurons and their sensory coding. Although several studies found that alterations of sensory information processing in the neocortex strongly correlate with state transitions, we were able to extend this correlation to the thalamocortical cells in the LGN. Additionally, our findings suggest that the visual evoked activity exhibited by TC cells can also be altered by state transitions in such way that while the pupil dilates, the orientation selectivity of TC neurons decreases. This seemingly counterintuitive phenomenon might be explained by the Yerkes-Dodson curve (Yerkes & Dodson, 1908) but the evidence for this requires rigorous experiments with longer epochs of all brain states and better segmentation thereof. Furthermore, the decrease in firing in putative LGN interneurons during AW does not necessarily mean that the net inhibition in TC neurons is decreased as some thalamic reticular neurons, the sources of a much larger inhibitory conductance (Bal, et al., 1995), are known to fire at much higher rates during AW (Halassa, et al., 2014).

What mechanisms are responsible for the differential arousal-dependent activity of LGN TC and interneurons? Our intracellular recordings in TC neurons reveal that during AW states the membrane potential of LGN TC neurons is less hyperpolarized than during QW, providing an explanation for the increases in FR during AW in LGN TC neurons. The firing mode of these neurons also changed from tonic to burst firing in the QW state, and in some cases, these bursts were characterized by a membrane potential polarization and interspike interval inconsistent with LTS-mediated burst firing, suggesting that they are high-threshold bursts similar to the ones recorded in the LGN of behaving cats (Hughes, et al., 2004; Lőrincz, et al., 2009b) and the somatosensory thalamus of lightly anesthetized mice (Crunelli, et al., 2012). Some of our extracellular recordings during QW clearly show LTS-mediated bursts (Fig. 12 B1), suggesting that high-threshold bursting is a property of a subset of LGN TC neurons as it was described in the cat LGN (Hughes, et al., 2004; Lőrincz, et al., 2009b; Lőrincz, et al., 2008). Importantly, we revealed a tight correlation between TC neuron membrane potential and pupil diameter, suggesting that the arousal-dependent membrane potential might originate from differential neuromodulation during AW and QW states. In line with this hypothesis, our findings suggest that local GABA release evoked by optogenetic activation of LH_{GABA} axons in the DRN

suppresses the activity of DRN_{GABA} neurons. This promotes wakefulness and occurs through a direct synaptic inhibition of DRN_{GABA} neurons mediated by $GABA_A$ receptors and leads to a prominent suppression of firing in DRN_{GABA} neurons *in vivo* (Gazea, et al., 2021). In our work, we showed that many DRN neurons slowly but persistently increase their activity upon photostimulation of LH_{GABA} axons in the DRN, presumably through the disinhibition of the local GABAergic neurons mentioned above.

Although multiple other brain sources could contribute to the modulation of LGN activity, the most prominent is likely to be corticothalamic fibers (Wilson, et al., 1984). Indeed, upon V1 inactivation, we found a prominent suppression of the arousal dependency of LGN TC neurons, suggesting that corticothalamic feedback is at least partly responsible for this phenomenon. Another important source of thalamic neuromodulation derives from the brainstem cholinergic nuclei (Varela & Sherman, 2007). If ACh is indeed involved in this arousal dependent modulation of thalamic neurons it could explain the differential arousal related behavior revealed here in TC neurons and interneurons, respectively. This is because whereas TC neurons are depolarized (McCormick & von Krosigk, 1992; Lőrincz, et al., 2008) LGN interneurons are hyperpolarized by ACh (McCormick & Pape, 1988). Thus, an increase in cholinergic tone during AW could explain both the increased TC neuron and decreased LGN interneuron firing. Neurons in the brainstem cholinergic nuclei show pronounced arousal dependent activity (Steriade, et al., 1990) making them a good candidate for mediating these effects. Taken together, our results show that the membrane potential and action potential output of LGN neurons are dynamically linked to arousal-dependent brain states in awake mice, although the functional implications of this phenomenon should be revealed by future studies.

8. CONCLUSIONS

In this thesis, substantial work has been done to explore the mechanism of visual information processing along with spontaneous activity of the mammalian brain. We focused primarily, but not exclusively, on brain function without artificial manipulation of its subnetworks, that is, we sought to answer questions like what the brain does, rather than what the brain can do. The latter question deals with problems that tend to happen only in highly controlled circumstances, seldom occur during the natural course of life. Instead, seeking to understand the phenomena happening in "real life" allows us to gain insights on more intricate aspects that almost everyone experiences in their daily activities, and provides basis for improving daily lives of ordinary people. Surely, studying diseases of the central nervous system has more clear-cut and imminent positive feedback on people's lives, but that is only one side of the coin. To deeply understand the inner workings our brains, we need more basis for comparing and contrasting pathological processes with physiological phenomena. Our work exemplifies this attitude and elucidates the default function of the visual system by providing evidence on brain state dependency of LGN neurons, and revealing the complexity of neuronal populations, thus stepping closer to the comprehensive description of how the visual system works as a network. Local GABAergic interneurons effectively shape network function in many, if not all, cortical and lower order subnetworks, and indirectly contribute to the concerted actions manifested in natural mammalian behavior. These brain state dependent mechanisms allow all mammalians (and probably other species too) to focus only on relevant environmental stimuli (i.e., increasing signal-to-noise ratio) while also conserving energy by reducing alertness in times where it is not needed. This evolutionary notion is in line with our findings, namely that the fluctuation of active and quiet awake states influences visual sensory processing by fine tuning the sensitivity to different environmental clues. Of course, this phenomenon has already been revealed by excellent scientist in the awake neocortex of mammals, but our work extended the scope of this mechanism to the visual thalamus, corroborating the idea that sensory processing occurs even at earlier stages of information flow. Not surprisingly, the neocortex exerts key regulatory action on this earlier stage, as we managed to point out, and this fact can be used as a counterargument for subcortical information processing, that is, neuronal regulation that happens below the cortex is also the working of the cortex if we inspect it as a whole network, however, we also know that subcortical sources of neuromodulatory chemicals have profound

effects on neocortical function (thus on downstream structures as well). The DRN, for example, is such a source, and as we explored the mechanisms thereof, we elucidated an intricate mutual connection with the lateral hypothalamus having a strong effect on promoting wakfulness from NREM sleep. This also makes sense in an evolutionary aspect, as the general hub that connects the homeostatic maintenance of the body itself with the surrounding environment has long been known to be the hypothalamus.

9. ACKNOWLEDGEMENTS

First and foremost, I would like to express my gratitude to my family, especially my parents who always supported me with kind and reassuring words when working in the laboratory, sometimes very late at the night in the weekends, became daunting. I am sure I could not have finished ever if it was not for them, and I can only hope that my father is proud of me who, very sadly, is not among us anymore and cannot see me finish my dissertation.

Naturally, I am thankful for my friends' support both from Szeged and Budapest, their unrelenting faith in me helped me immeasurably to cope with the difficulties of PhD, and I know I can always count on them, even if not in strictly professional matters.

I would also like to thank my colleagues in and outside our lab, their keen professional observations and help made many experiments easier, or possible at all. I am especially thankful for Gáspár Oláh, not only because his solutions were pinnacles of innovation but also because he had the patience to explain everything about electrophysiology simply and clearly.

Finally, I thank the head of Biology Doctoral School, Prof. Dr. Csaba Vágvölgyi, for my admission to the PhD program, and my supervisor, Dr. Magor L. Lőrincz, this opportunity of PhD and his views on either scientific or non-scientific matters that helped me see the world through different lenses.

10. REFERENCES

Allers, K. & Sharp, T., 2003. Neurochemical and anatomical identification of fast- and slow neurones in the rat dorsal raphe nucleus using juxtacellular labelling methods in vivo. *Neuroscience,* Volume 122, pp. 193-204.

Amzica, F. & Steriade, M., 1995. Short- and long-range neuronal synchronization of the slow (< 1 Hz) cortical oscillation. *Journal of Neurophysiology,* Volume 73(1), pp. 20-38..

Aserinsky, E. & Kleitman, N., 1953. Regularly occurring periods of eye motility, and concomitant phenomena during sleep. *Science,* Volume 118, p. 273–4.

Aydın, Ç. et al., 2018. Locomotion modulates specific functional cell types in the mouse visual thalamus. *Nat Commun,* Volume 9(1), p. 4882.

Bal, T. & McCormick, D. A., 1993. Mechanisms of oscillatory activity in guinea-pig nucleus reticularis thalami in vitro: a mammalian pacemaker. *The Journal of Physiology,* Volume 468, pp. 669-691.

Bal, T., von Krosigk, M. & McCormick, D. A., 1995. Role of the ferret perigeniculate nucleus in the generation of synchronized oscillations in vitro. *The Journal of Physiology,* Volume 483.

Bal, T., von Krosigk, M. & McCormick, D. A., 1995. Synaptic and membrane mechanisms underlying synchronized oscillations in the ferret lateral geniculate nucleus in vitro. *The Journal of Physiology,* Volume 483.

Bennett, C., Arroyo, S. & Hestrin, S., 2013. Subthreshold mechanisms underlying state-dependent modulation of visual responses. *Neuron,* Volume 80, pp. 350-357.

Berger, H., 1929. Über das Elektrenkephalogramm des Menschen. *Archiv f. Psychiatrie,* Volume 87, pp. 527-570.

Bezdudnaya, T. et al., 2006. Thalamic burst mode and inattention in the awake LGNd. *Neuron,* Volume 49, p. 421–432.

Bollimunta, A., Mo, J., Schroeder, C. & Ding, M., 2011. Neuronal mechanisms and attentional modulation of corticothalamic α oscillations. *J Neurosci,* Volume 31(13), pp. 4935-43.

Bonnavion, P. et al., 2016. Hubs and spokes of the lateral hypothalamus: cell types, circuits and behaviour. *The Journal of Physiology,* Volume 594, pp. 6443-6462.

Boyd, A. M., Sturgill, J. F. & Poo, C. &. I. J. S., 2012. Cortical feedback control of olfactory bulb circuits. *Neuron,* Volume 76(6), p. 1161–1174.

Carandini, M. & Ferster, D., 1997. A tonic hyperpolarization underlying contrast adaptation in cat visual cortex. *Science,* Volume 276, pp. 949-52.

Cardin, J. et al., 2009. Driving fast-spiking cells induces gamma rhythm and controls sensory responses.. *Nature,* Volume 459(7247), pp. 663-7.

Carracedo, L. et al., 2013. A Neocortical Delta Rhythm Facilitates Reciprocal Interlaminar Interactions via Nested Theta Rhythms. *Journal of Neuroscience,* Volume 33, pp. 10750-10761.

Cheong, S., Tailby, C., Solomon, S. & Martin, P., 2013. Cortical-like receptive fields in the lateral geniculate nucleus of marmoset monkeys. *J Neurosci,* Volume 33(16), pp. 6864-7.

Constantinople, C. & Bruno, R., 2011. Effects and Mechanisms of Wakefulness on Local Cortical Networks. *Neuron,* Volume 69, pp. 1061-1068.

Contreras, D. &. S. M., 1996. Spindle oscillation in cats: the role of corticothalamic feedback in a thalamically generated rhythm. *J. Physiol,* Volume 490, p. 159–179.

Covington, B. & Al Khalili, Y., 2021. Neuroanatomy, Nucleus Lateral Geniculate. *StatPearls Publishing,* Issue https://www.ncbi.nlm.nih.gov/books/NBK541137/.

Crochet, S. & Petersen, C. C. H., 2006. Correlating whisker behavior with membrane potential in barrel cortex of awake mice. *Nature Neuroscience ,* Volume 9, pp. 608-610.

Crunelli, V., Lorincz, M. L., Errington, A. C. & Hughes, S. W., 2012. Activity of cortical and thalamic neurons during the slow (<1 Hz) rhythm in the mouse in vivo. *Pflugers Archiv : European journal of physiology,* Volume 463, pp. 73-88.

Crunelli, V. et al., 2018. Dual function of thalamic low-vigilance state oscillations: rhythm-regulation and plasticity. *Nature Reviews Neuroscience,* Volume 19, pp. 107-118.

Crunelli, V. et al., 2004. The 'window' T-type calcium current in brain dynamics of different behavioural states. *Journal of Physiology,* Volume 562, p. 121–129.

Dawson, G. & Walter, W., 1945. Recommendations for the design and performance of electroencephalographic apparatus.. *Journal of Neurology Neurosurgery & Psychiatry,* Volume 8(3-4), pp. 61-64.

Dolabela de Lima, A., Montero, V. & Singer, W., 1985. The cholinergic innervation of the visual thalamus: an EM immunocytochemical study. *Experimental Brain Research,* Volume 59, pp. 206-212.

Dossi, R., Nuñez, A. & Steriade, M., 1992. Electrophysiology of a slow (0.5-4 Hz) intrinsic oscillation of cat thalamocortical neurones in vivo. *J Physiol,* Volume 447, pp. 215-34.

Dougherty, K. et al., 2015. Ongoing Alpha Activity in V1 Regulates Visually Driven Spiking Responses. *Cerebral Cortex,* Volume 27, pp. 1113-24.

Eggermann, E., Kremer, Y., Crochet, S. & Petersen, C., 2014. Cholinergic Signals in Mouse Barrel Cortex during Active Whisker Sensing. *Cell Reports,* Volume 9, pp. 1654-1660.

Einstein, M. C., Polack, P.-O., Tran, D. T. & Golshani, P., 2017. Visually Evoked 3–5 Hz Membrane Potential Oscillations Reduce the Responsiveness of Visual Cortex Neurons in Awake Behaving Mice. *J. Neurosci.,* Volume 37, pp. 5084-5098.

Engel, A., Fries, P. & & Singer, W., 2001. Dynamic predictions: Oscillations and synchrony in top–down processing. *Nat Rev Neurosci,* Volume 2, p. 704–716.

Fonyó, A., 2011. Az orvosi élettan tankönyve. *Medicina Könyvkiadó Zrt.,* p. 647.

Fox, M. D. & Raichle, M. E., 2007. Spontaneous fluctuations in brain activity observed with functional magnetic resonance imaging. *Nat Rev Neurosci,* Volume 8, pp. 700-11.

Friedlander, M. J., Lin, C. S., Stanford, L. R. & Sherman, S. M., 1981. Morphology of functionally identified neurons in lateral geniculate nucleus of the cat. *J Neurophysiol,* Volume 46(1), pp. 80-129.

Gazea, M. et al., 2021. Reciprocal Lateral Hypothalamic and Raphe GABAergic Projections Promote Wakefulness. *J Neurosci.,* Volume 41, pp. 4840-4849.

Gent, T. C., Bassetti, C. L. & Adamantidis, A. R., 2018. Sleep-wake control and the thalamus. *Current Opinion in Neurobiology,* Volume 52, pp. 188-197.

Gilzenrat, M. S., Nieuwenhuis, S., Jepma, M. & & Cohen, J. D., 2010. Pupil diameter tracks changes in control state predicted by the adaptive gain theory of locus coeruleus function.. *Cognitive, affective & behavioral neuroscience,* Volume 10, pp. 252-269.

Haas, L. F., 2003. Hans Berger (1873–1941), Richard Caton (1842–1926), and electroencephalography. *Journal of Neurology, Neurosurgery & Psychiatry,* Volume 74, p. 9.

Haegens, S. et al., 2011. α-Oscillations in the monkey sensorimotor network influence discrimination performance by rhythmical inhibition of neuronal spiking. *Proc Natl Acad Sci USA,* Volume 108, pp. 19377-82.

Haider, B., Michael Häusser, M. & Carandini, M., 2013. Inhibition dominates sensory responses in awake cortex. *Nature,* 493(7430), pp. 97-100.

Halassa, M. et al., 2014. State-dependent architecture of thalamic reticular subnetworks.. *Cell,* Volume 158, p. 808–821.

Halgren, M. et al., 2019. The generation and propagation of the human alpha rhythm. *Proc Natl Acad Sci USA,* Volume 116, pp. 23772-23782.

Hassani, O., Henny, P., Lee, M. & Jones, B., 2010. GABAergic neurons intermingled with orexin and MCH neurons in the lateral hypothalamus discharge maximally during sleep.. *Eur. J. Neurosci,* Volume 32, p. 448–457.

Herrera, C., Cadavieco, M. & Jego, S. e. a., 2016. Hypothalamic feedforward inhibition of thalamocortical network controls arousal and consciousness. *Nature Neuroscience,* Volume 16, p. 290–298.

Herrero, M., Barcia, C. & Navarro, J., 2002. Functional anatomy of thalamus and basal ganglia. *Childs Nerv Syst,* Volume 18, p. 386–404.

Hirsch, J. C., Fourment, A. & Marc, M. E., 1983. Sleep-related variations of membrane potential in the lateral geniculate body relay neurons of the cat. *Brain research,* Volume 259, pp. 308-312.

Hodgkin, A. L. & Huxley, A. F., 1939. Action Potentials Recorded from Inside a Nerve Fibre. *Nature,* Volume 144, pp. 710-711.

Holdefer, R. & Jacobs, B., 1994. Phasic stimulation of the locus coeruleus: effects on activity in the lateral geniculate nucleus. *Exp Brain Res,* Volume 100(3), pp. 444-52.

Hughes, S. et al., 1999. All thalamocortical neurones possess a T-type Ca2+ 'window' current that enables the expression of bistability-mediated activities. *Journal of Physiology,* Volume 517, pp. 805-15.

Hughes, S. & Crunelli, V., 2005. Thalamic Mechanisms of EEG Alpha Rhythms and Their Pathological Implications. *The Neuroscientist,* Volume 11, p. 357.

Hughes, S., Lorincz, M., Parri, H. & Crunelli, V., 2011. Infraslow (<0.1 Hz) oscillations in thalamic relay nuclei basic mechanisms and significance to health and disease states. *Prog Brain Res,* Volume 193, pp. 145-62.

Hughes, S. et al., 2004. Synchronized oscillations at alpha and theta frequencies in the lateral geniculate nucleus. *Neuron,* Volume 42, pp. 253-268.

Hughes, S. W., Cope, D. W., Blethyn, K. L. & Crunelli, V., 2002. Cellular mechanisms of the slow (<1 Hz) oscillation in thalamocortical neurons in vitro. *Neuron,* Volume 33, pp. 947-958.

Jahnsen, H. & Llinas, R., 1984. Electrophysiological properties of guinea-pig thalamic neurones: an in vitro study. *The Journal of physiology,* Volume 349, pp. 205-226.

Jahnsen, H. & Llinas, R., 1984. Voltage-dependent burst-to-tonic switching of thalamic cell activity: an in vitro study. *Archives italiennes de biologie,* Volume 122, pp. 73-82.

Kahneman, D. & Beatty, J., 1966. Pupil diameter and load on memory. *Science,* Volume 154, pp. 1583-5.

Kravitz, D., Saleem, K., Baker, C. & Mishkin, M., 2011. A new neural framework for visuospatial processing. *Nat Rev Neurosci,* Volume 2(4), pp. 217-30.

Krueger, J. & Disney, A., 2019. Structure and function of dual-source cholinergic modulation in early vision. *J Comp Neurol,* Volume 527(3), pp. 738-750.

Lakatos, P. et al., 2008. Entrainment of Neuronal Oscillations as a Mechanism of Attentional Selection. *Science,* Volume 320, pp. 110-113.

Larkum, M. E. et al., 2009. Synaptic Integration in Tuft Dendrites of Layer 5 Pyramidal Neurons: A New Unifying Principle. *Science ,* Volume 325, pp. 756-760.

Lemieux, M. et al., 2014. The impact of cortical deafferentation on the neocortical slow oscillation. *J Neurosci,* Volume 34, pp. 5689-703.

Leresche, N. et al., 1991. Low-frequency oscillatory activities intrinsic to rat and cat thalamocortical cells. *The Journal of Physiology,* Volume 441.

Leresche, N. et al., 1991. Low-frequency oscillatory activities intrinsic to rat and cat thalamocortical cells.. *Journal of Physiology,* Volume 441, pp. 155-174.

Livingstone, M. S. & Hubel, D. H., 1981. Effects of sleep and arousal on the processing of visual information in the cat. *Nature,* Volume 291, p. 554–561.

Llinás, R. & Jahnsen, H., 1982. Electrophysiology of mammalian thalamic neurones in vitro. *Nature,* Volume 297, p. 406–408.

Lopes Da Silva, F. & Storm Van Leeuwen, W., 1977. The cortical source of the alpha rhythm. *Neuroscience Letters,* Volume 6, pp. 237-241.

Lopes da Silva, F., Vos, J., Mooibroek, J. & van Rotterdam, A., 1980. Relative contributions of intracortical and thalamo-cortical processes in the generation of alpha rhythms, revealed by partial coherence analysis. *Electroencephalography and Clinical Neurophysiology,* Volume 50, pp. 449-456.

Lottem, E., Lörincz, M. & ZF., M., 2016. Optogenetic Activation of Dorsal Raphe Serotonin Neurons Rapidly Inhibits Spontaneous But Not Odor-Evoked Activity in Olfactory Cortex. *J Neurosci.,* Volume 36(1), pp. 7-18.

Lowry, C. et al., 2008. Serotonergic systems, anxiety, and affective disorder: focus on the dorsomedial part of the dorsal raphe nucleus.. *Annals of the New York Academy of Sciences,* Volume 1148, pp. 86-94.

Lozano-Soldevilla, et al., 2014. GABAergic modulation of visual gamma and alpha oscillations and its consequences for working memory performance. *Curr Biol,* Volume 24(24), pp. 2878-87.

Lőrincz, M., Crunelli, V. & Hughes, S., 2008. Cellular dynamics of cholinergically-induced alpha (8-13 Hz) rhythms in sensory thalamic nuclei in vitro. *Journal of Neuroscience,* Volume 28, p. 660–671.

Lőrincz, M. et al., 2015. A distinct class of slow (~0.2-2 Hz) intrinsically bursting layer 5 pyramidal neurons determines UP/DOWN state dynamics in the neocortex. *J Neurosci,* Volume 35(14), pp. 5442-58.

Lőrincz, M. et al., 2009. ATP-Dependent Infra-Slow (<0.1 Hz) Oscillations in Thalamic Networks. *PLoS One,* Volume 4, p. e4447.

Lőrincz, M. L. & Adamantidis, A. R., 2017. Monoaminergic control of brain states and sensory processing: Existing knowledge and recent insights obtained with optogenetics. *Progress in Neurobiology,* Volume 151, pp. 237-253.

Lőrincz, M. L. et al., 2009. Temporal framing of thalamic relay-mode firing by phasic inhibition during the alpha rhythm. *Neuron,* Volume 63, pp. 683-696.

Lőrincz, M. L., Lottem, E. & Mainen, Z. F., 2016. Optogenetic Activation of Dorsal Raphe Serotonin Neurons Rapidly Inhibits Spontaneous But Not Odor-Evoked Activity in Olfactory Cortex. *Journal of Neuroscience,* Volume 36, pp. 7-18.

Massimini, M. et al., 2005. Breakdown of cortical effective connectivity during sleep.. *Science,* Volume 309, pp. 2228-32.

McCormick, D. A., 1993. Chapter 36: Actions of acetylcholine in the cerebral cortex and thalamus and implications for function. *Progress in Brain Research,* Volume 98, pp. 303-308.

McCormick, D. A. & Bal, T., 1997. Sleep and arousal: thalamocortical mechanisms. *Annual review of neuroscience,* Volume 20, pp. 185-215.

McCormick, D. A., McGinley, M. J. & Salkoff, D. B., 2015. Brain state dependent activity in the cortex and thalamus. *Curr Opin Neurobiol,* Volume 31, pp. 133-140.

McCormick, D. A. & Pape, H.-C., 1988. Acetylcholine inhibits identified interneurons in the cat lateral geniculate nucleus. *Nature,* Volume 334, pp. 246-248.

McCormick, D. A. & von Krosigk, M., 1992. Corticothalamic activation modulates thalamic firing through glutamate "metabotropic" receptors. *PNAS,* Volume 89(7), pp. 2774-2778.

McCormick, D. & Pape, H., 1990. Properties of a hyperpolarization-activated cation current and its role in rhythmic oscillation in thalamic relay neurones. *J Physiol,* Volume 431, pp. 291-318.

McCormick, D. & Prince, D. A., 1987 . Actions of acetylcholine in the guinea-pig and cat medial and lateral geniculate nuclei, in vitro. *J Physiol.,* Volume 392, pp. 147-65.

McGinley, M. J. et al., 2015. Waking State: Rapid Variations Modulate Neural and Behavioral Responses. *Neuron,* Volume 87, pp. 1143-1161.

McGinley, M. J., S V, D. & McCormick, D. A., 2015. Cortical Membrane Potential Signature of Optimal States for Sensory Signal Detection. *Neuron,* Volume 87, pp. 179-192.

Miyazaki, K. et al., 2014. Optogenetic activation of dorsal raphe serotonin neurons enhances patience for future rewards. *Curr Biol.,* Volume 24(17), pp. 2033-40.

Monckton, J. E. & McCormick, D. A., 2002. Neuromodulatory Role of Serotonin in the Ferret Thalamus. *Journal of Neurophysiology,* Volume 87, pp. 2124-36.

Montero, V., 1991. A quantitative study of synaptic contacts on interneurons and relay cells of the cat lateral geniculate nucleus. *Experimental Brain Research,* Volume 86, p. 257–270.

Moore, R. & Card, J., 1994. Intergeniculate leaflet: an anatomically and functionally distinct subdivision of the lateral geniculate complex. *J Comp Neurol,* Volume 344, pp. 403-30.

Motokawa, K. & Suzuki, H., 1966. Central mechanism of vision. *Progress in brain research,* Volume 21, pp. 163-179.

Murphy, P., Duckett, S. G. & Sillito, A., 1999. Feedback connections to the lateral geniculate nucleus and cortical response properties.. *Science,* Volume 286(5444), pp. 1552-4..

Nevian, T., Larkum, M. & Polsky, A. e. a., 2007. Properties of basal dendrites of layer 5 pyramidal neurons: a direct patch-clamp recording study. *Nat Neurosci,* Volume 10, p. 206–214.

Niedermeyer, E. & Lopes Da Silva, F., 2004. Electroencephalography: Basic Principles, Clinical Applications, and Related Fields. *Lippincott Williams Wilkins.*

Niell, C. & Stryker, M., 2010. Modulation of visual responses by behavioral state in mouse visual cortex.. *Neuron,* Volume 65, p. 472–479.

Petersen, C. & Crochet, S., 2013. Synaptic Computation and Sensory Processing in Neocortical Layer 2/3. *Neuron,* Volume 78, pp. 28-48.

Pinault, D., 1996. A novel single-cell staining procedure performed in vivo under electrophysiological control: morpho-functional features of juxtacellularly labeled thalamic cells and other central neurons with biocytin or Neurobiotin. *Journal of Neuroscience methods,* Volume 65, pp. 113-136.

Polack, P. O., Friedman, J. & Golshani, P., 2013. Cellular mechanisms of brain state-dependent gain modulation in visual cortex. *Nature neuroscience,* pp. 1331-1339.

Poulet, J., Fernandez, L., Crochet, S. & Petersen, C., 2012. Thalamic control of cortical states. *Nature Neuroscience,* Volume 15, p. 370–372.

Poulet, J. F. & Petersen, C. C., 2008. Internal brain state regulates membrane potential synchrony in barrel cortex of behaving mice. *Nature,* Volume 454, pp. 881-885.

Reimer, J. et al., 2014. Pupil fluctuations track fast switching of cortical states during quiet wakefulness. *Neuron,* Volume 84, pp. 355-362.

Reimer, J. et al., 2016. Pupil fluctuations track rapid changes in adrenergic and cholinergic activity in cortex. *Nature Communications,* Volume 7, p. 13289.

Scheffzük, C. et al., 2011. Selective Coupling between Theta Phase and Neocortical Fast Gamma Oscillations during REM-Sleep in Mice.. *PLoS One,* Volume 6(12), p. e28489.

Senzai, Y., Fernandez-Ruiz, A. & Buzsáki, G., 2019. Layer-Specific Physiological Features and Interlaminar Interactions in the Primary Visual Cortex of the Mouse. *Neuron,* Volume 101, pp. 500-513.

Sherman, S. & Guillery, R., 2002. The role of the thalamus in the flow of information to the cortex. *Philos Trans R Soc Lond B Biol Sci,* Volume 357(1428), pp. 1695-708.

Sherman, S. M. & Guillery, R., 1998. On the actions that one nerve cell can have on another: Distinguishing “drivers” from “modulators”. *PNAS,* Volume 95 (12), pp. 7121-7126.

Staudigl, T. et al., 2017. Saccades are phase-locked to alpha oscillations in the occipital and medial temporal lobe during successful memory encoding. *PLoS Biol,* Volume 15(12), p. e2003404.

Steriade, M., 1978. Cortical long-axoned cells and. *THE BEHAVIORAL AND BRAIN SCIENCES,* Volume 3, pp. 465-514.

Steriade, M., Contreras, D., Curró Dossi, R. & A., N., 1993. The slow (< 1 Hz) oscillation in reticular thalamic and thalamocortical neurons: scenario of sleep rhythm generation in interacting thalamic and neocortical networks. *J Neurosci,* Volume 13, pp. 3284-99.

Steriade, M. et al., 1990. Neuronal activities in brain-stem cholinergic nuclei related to tonic activation processes in thalamocortical systems. *J. Neurosci,* Volume 10, pp. 2541-59.

Steriade, M., Deschenes, M., Domich, L. & Mulle, C., 1985. Abolition of spindle oscillations in thalamic neurons disconnected from nucleus reticularis thalami. *Journal of Neurophysiology,* Volume 54:6, pp. 1473-1497.

Steriade, M., Nunez, A. & Amzica, F., 1993. A novel slow (< 1 Hz) oscillation of neocortical neurons in vivo: depolarizing and hyperpolarizing components. *Journal of Neuroscience,* Volume 13, pp. 3252-3265.

Steriade, M., Timofeev, I. & Grenier, F., 2001. Natural Waking and Sleep States: A View From Inside Neocortical Neurons. *Journal of Neurophysiology,* Volume 85(5), pp. 1969-85.

Taniguchi, H., 2014. Genetic dissection of GABAergic neural circuits in mouse neocortex. *Front Cell Neurosci,* Volume 8, p. 8.

Thevenaz, P. & Unser, M., 2008. Snakuscules. *IEEE Trans Image Process,* Volume 17, p. 585–593.

Timofeev, I. & Steriade, M., 1996. Low-frequency rhythms in the thalamus of intact-cortex and decorticated cats. *J Neurophysiol,* Volume 76, pp. 4152-68.

Traub, R., Hawkins, K. & Adams, N. e. a., 2020. Layer 4 pyramidal neuron dendritic bursting underlies a post-stimulus visual cortical alpha rhythm. *Commun Biol,* Volume 3, p. 230 .

Vanhatalo, S. et al., 2004. Infraslow oscillations modulate excitability and interictal epileptic activity in the human cortex during sleep. *Proc Natl Acad Sci USA,* Volume 101, p. 5053–5057.

Varela, C. & Sherman, S., 2007. Differences in response to muscarinic activation between first and higher order thalamic relays. *J Neurophysiol,* Volume 98, pp. 3538-47.

Vinck, M., Batista-Brito, R., Knoblich, U. & Cardin, J. A., 2015. Arousal and locomotion make distinct contributions to cortical activity patterns and visual encoding. *Neuron,* Volume 86, pp. 740-754.

Vlisides, P. et al., 2018. Subanaesthetic ketamine and altered states of consciousness in humans. *Br J Anaesth,* Volume 121, pp. 249-259.

Vong, L. et al., 2011. Leptin action on GABAergic neurons prevents obesity and reduces inhibitory tone to POMC neurons. *Neuron,* Volume 71, pp. 142-154.

Wilson, J., Friedlander, M. & Sherman, S., 1984. Fine structural morphology of identified X- and Y-cells in the cat's lateral geniculate nucleus. *Proc R Soc Lond B Biol Sci,* Volume 221, p. 411–436.

Yerkes, R. M. & Dodson, J. D., 1908. THE RELATION OF STRENGTH OF STIMULUS TO RAPIDITY OF HABIT-FORMATION. *Journal of Comparative Neurology and Psychology,* Volume 18, pp. 459-482.

Yoshida, M., Sasa, M. & Takaori, S., 1984. Serotonin-mediated inhibition from dorsal raphe nucleus of neurons in dorsal lateral geniculate and thalamic reticular nuclei. *Brain Res,* Volume 290(1), pp. 95-105.

Zagha, E. et al., 2013. Motor cortex feedback influences sensory processing by modulating network state. *Neuron,* Volume 79, pp. 567-578.

ABSTRACT

Brain state dependent thalamocortical (TC) activity plays and important role in sensory coding, oscillations and cognition. The lateral geniculate nucleus (LGN) relays visual information to the cortex, but the state dependent spontaneous and visually evoked activity of LGN neurons in awake behaving animals remains controversial. In awake head-restrained mice, using a combination of pupillometry, extracellular and intracellular recordings from morphologically and physiologically identified LGN neurons we show that TC neurons and putative local interneurons are inversely related to arousal forming two complementary coalitions with TC cells being positively correlates with wakefulness, while local interneuron activity is negatively correlated. Additionally, the orientation tuning of visually evoked thalamic cell responses is altered during various brain states. Intracellular recordings indicated that the membrane potential of LGN TC neurons was tightly correlated to fluctuations in pupil size. Inactivating the corticothalamic feedback by $GABA_A$ agonist muscimol applied on the dural surface significantly diminishes the correlation between brain states and thalamic neuronal activity. Additional investigations show that by photostimulating GABAergic axons (expressing Channelrhodopsin-2 in a Cre-dependent manner) that project from the lateral hypothalamus (LH) to the dorsal raphe nucleus (DRN), neurons in the DRN increase their action potential output, presumably through disinhibition. Taken together our results show that LGN neuronal membrane potential and action potential output are dynamically linked to arousal dependent brain states in awake mice and this fact might have important functional implications.

ÖSSZEFOGLALÓ

Az agyiállapot-függő talamokortikális (TC) sejtaktivitás fontos szerepet játszik a szenzoros kódolásban, illetve agyi oszcillációkban és kognícióban. A corpus geniculatum laterale (CGL) közvetíti a vizuális információt az agykéregbe, ám a CGL állapotfüggő spontán aktivitása, ill. a vizuális kiváltott válaszai éber állatokban egyelőre nem egyértelműek. Éber, fejbefogott egerek morfológiailag és élettanilag beazonosított CGL-neuronjaiban történő pupillometriai, extracelluláris és intracelluláris mérések kombinációjából kiderül, hogy a TC-sejtek és a valószínűsíthetően lokális interneuronok fordított viszonyban vannak egymással az éberség szintjétől függően, és így egy egymást kiegészítő koalíciót képeznek. Míg a TC-neuronok aktivitása pozitívan korrelált az éberség szintjével, addig az lokális interneuronok negatívan korreláltak. Ezen kívül a talamikus sejtek vizuális kiváltott válaszainak az orientációs finomhangolása megváltozik az agyi állapotok hullámzásával. Az intracelluláris elvezetések alapján kimutattuk, hogy CGL TC-sejtjeinek membránpotenciálja szoros korrelációt mutatnak a pupillaátmérő változásaival. A kortikotalamikus visszacsatolás inaktiválásakor, amit a muscimol nevű $GABA_A$-receptor agonista alkalmazásával értünk el a dura mater felületén, szignifikánsan csökken a korreláció az agyi állapotok és a talamikus sejtek aktivitása között. További kísérleteink alapján a laterális hypothalamusból (LH) a nucleus raphe dorsalisba (NRD) érkező GABAerg axonok fotostimulációja (Cre-dependens Channelrhodopsin-2 expressziója révén) növeli az NRD sejtjeinek a tüzelését, feltételezhetően diszinhibíción keresztül. Eredményeinket összefoglalva elmondható, hogy a CGL neuronjainak membránpotenciálja és tüzelése dinamikusan kapcsolódik az agyi állapotok váltakozásaihoz éber egerekben, aminek a funkcionális relevanciája számottevő lehet a jövőben.